Macrozooplankton and micronekton diversity and associated carbon vertical patterns and fluxes under distinct productive conditions around the Kerguelen Islands

Cotté Cedric [1, 2, *], Ariza A. [3], Berne Adrien [1, 2], Habasque Jeremie [2], Lebourges-Dhaussy Anne [2], Roudaut Gildas [2], Espinasse B. [4], Hunt B.P.V. [5, 6, 7], Pakhomov E.A. [5, 6, 7], Henschke N. [5], Péron C. [8], Conchon A. [1, 2], Koedooder C. [9, 10], Izard L. [1], Cherel Y. [11]

[1] Sorbonne Université, CNRS, IRD, MNHN, Laboratoire d'Océanographie et du Climat: Expérimentations et Approches Numériques (LOCEAN-IPSL), Paris, France
[2] LEMAR, UBO-CNRS-IRD-Ifremer IUEM, Plouzané, France c MARBEC, Univ. Montpellier, CNRS, Ifremer, IRD, Sète, France
[3] MARBEC, Univ. Montpellier, CNRS, Ifremer, IRD, Sète, France
[4] Department of Arctic and Marine Biology, UiT The Arctic University of Norway, Tromsø, Norway
[5] Department of Earth, Ocean and Atmospheric Sciences, University of British Columbia, Vancouver, British Columbia, Canada
[6] Institute for the Oceans and Fisheries, University of British Columbia, Vancouver, British Columbia, Canada
[7] Hakai Institute, PO Box 309, Heriot Bay, BC, Canada
[8] BOREA, MNHN- CNRS-UPMC-IRD-UCBN-UAG, Paris, France
[9] Sorbonne Université, UPMC Univ Paris 06, CNRS, Laboratoire d'Océanographie Microbienne (LOMIC), Observatoire Océanologique, Banyuls/mer, France
[10] The Fredy and Nadine Herrmann Institute of Earth Sciences, Hebrew University of Jerusalem, Jerusalem, Israel
[11] Centre d'Etudes Biologiques de Chizé (CEBC), UMR 7372 du CNRS-La Rochelle Université, 79360 Villiers-en-Bois, France

* Corresponding author : Cedric Cotté, email address : cedric.cotte@locean.ipsl.fr

Abstract :

Mesopelagic communities are characterized by a large biomass of diverse macrozooplankton and micronekton (MM) performing diel vertical migration (DVM) connecting the surface to the deeper ocean and contributing to biogeochemical fluxes. In the Southern Ocean, a prominent High Nutrient Low Chlorophyll (HNLC) and low carbon export region, the contribution of MM to the vertical carbon flux of the biological pump remains largely unknown. Furthermore, few studies have investigated MM communities and vertical flux in naturally iron fertilized areas associated with shallow bathymetry. In this study, we assessed the MM community diversity, abundance and biomass in the Kerguelen Island region, including two stations in the HNLC region upstream of the islands, and two stations in naturally iron fertilized areas, one on the Plateau, and one downstream of the Plateau. The MM community was examined using a combination of trawl sampling and acoustic measurements at 18 and 38 kHz from the surface to 800 m. A conspicuous three-layer vertical system was observed in all areas - a shallow scattering layer, SSL, between 10 and 200 m; mid-depth scattering layer, MSL, between 200 and 500 m; deep scattering layer,

DSL, between 500 and 800 m - but communities differing among stations. While salps (Salpa thompsoni) dominated the biomass at the productive Kerguelen Plateau and the downstream station, they were scarce in the HNLC upstream area. In addition, crustaceans (mainly Euphausia vallentini and Themisto gaudichaudii) were particularly abundant over the Plateau, representing a large, although varying, carbon stock in the 0–500 m water layer. Mesopelagic fish were prominent below 400 m where they formed permanent or migrant layers accounting for the main source of carbon biomass. Through these spatial and temporal sources of variability, complex patterns of the MM vertical distribution and associated carbon content were identified. The total carbon flux mediated by migratory myctophids at the four stations was quantified. While this flux was likely underestimated, this study identified the main components and mechanisms of active carbon export in the region and how they are modulated by complex topography and land mass effects.

Highlights

► This Study reports a detailed description of the macrozooplankton and micronekton communities in the Kerguelen area using trawl and two-frequency acoustic data ► We depict a consistent three-layers system observed between the surface and 800 m over the Kerguelen seascape (Chlorophyll biomass, Polar Front position) but different assemblages ► Salps was dominant in terms of biomass in the productive areas and scarce in HNLC region while crustaceans were abundant on the Plateau ► Myctophids were prominent below 400 m where they formed permanent or migrant layers accounting for the main source of carbon biomass ► We estimate total carbon flux mediated by migratory myctophids in the contrasting productive areas

Introduction

The mesopelagic community is composed of taxonomically and functionally diverse groups of organisms, including gelatinous organisms, crustaceans and mesopelagic fish, that occupy the 200-1000 m depth zone in the ocean. Through modelling and *in-situ* studies, mesopelagic organisms have gained increasing attention from the ecological and biogeochemical communities (Davison et al., 2013, Anderson et al., 2018, Hernández-León et al., 2019) and from managers interested in the sustainable exploitation of potential new resources (Grimaldo et al., 2020). This interest has primarily been stimulated by two characteristics of the mesopelagic zooplankton and micronekton. First, while logistical and technological difficulties in reliably estimating zooplankton and fish biomass still exist, recent assessments have pointed to a high likelihood of these populations being substantially underestimated (Irigoien et al., 2014, Hernández-León et al., 2020). Secondly, mesopelagic organisms are known to perform extensive diel vertical migration (DVM, described as the largest animal migration on Earth (Longhurst, 1976; Behrenfeld et al., 2019), between the mesopelagic zone (200-1000 m) during the day and the epipelagic zone (0-200 m) to feed at night.. This vertical movement connects the mesopelagic and epipelagic zones and represents an important active contribution in the downward flux of organic matter, and particularly the export of carbon to the deep ocean (Bianchi et al., 2013; Ariza et al., 2015).

The Southern Ocean is the world ocean's largest high nutrient low chlorophyll (HNLC) area where the primary production is mainly limited by iron (de Baar et al., 1995). Naturally iron-fertilized sites generate highly productive regions in the Southern Ocean (Blain et al., 2007). The Kerguelen Plateau forms a large physical barrier to the eastward flowing Antarctic Circumpolar Current (ACC) and induces iron enrichment of shelf waters that are entrained in the downstream area eastward of the Plateau (Blain et al., 2007, Mongin et al., 2008). While upstream waters approaching the Kerguelen Islands are generally depleted in iron and chlorophyll (Jandel et al., 1998), a large bloom occurs over the Kerguelen Plateau as well as in the downstream region, observed as temporally persistent (over the spring and early summer period) and spatially dynamic high-chlorophyll plume (d'Ovidio et al., 2015). While these productive areas contribute to the sink of atmospheric CO_2 through photosynthesis , an inverse relationship has been observed between production and particulate carbon flux in the Kerguelen area (Savoye et al., 2008), which has also been observed elsewhere in the Southern Ocean (Maiti et al., 2013, Le Moigne et al., 2016). However, to date research has focussed on passive carbon flux in this region, and the contribution of active carbon flux remains unresolved. Given the prominent role of the

Southern Ocean in the global carbon cycle, active carbon flux needs to be addressed to assess the contribution of the active migrating community of organisms. This community includes a large variety of macrozooplankton and micronekton (MM) performing DVMs of variable magnitudes (e.g., Roe et al., 1984). The knowledge gap of their role in ecosystems, including the diversity and contribution in biogeochemical stocks and flux, has recently been stressed (Ratnarajah et al., 2020, Martin et al., 2020).

The Kerguelen area (i.e., the Plateau and surrounding upstream and downstream waters) offers ideal conditions to investigate the diversity of pelagic ecosystems and the associated active biological pump at a site of natural iron fertilization and contrasting production regimes. This region is also ecologically important as a foraging ground for several species of land-based marine top predators often used as bioindicators of productive areas and rich trophic webs (Hindel et al., 2011). Their diet is largely comprised of MM and the estimated food consumption by the highest trophic level predators indicates the presence of significant standing stock of mesopelagic micronekton, primarily myctophids, and macrozooplankton, including euphausiids and hyperiids (Guinet et al., 1996, Bocher et al., 2001, Bost et al., 2002, Cherel et al., 2002, Lea et al., 2002, Cherel et al., 2008). In this subantarctic area of the Southern Ocean, high abundances of intermediate trophic levels have been reported in association with either circumpolar frontal regions or local bathymetry-driven features (Pakhomov et al., 1994, Pakhomov and Froneman 1999, Behagle et al., 2017). For instance, the abundance of the subantarctic krill E*uphausia vallentini* was associated with the shelf topography and the location of the Polar Front, and it was reported to be more numerous in the eastern area than in the western part of the Kerguelen region (Koubbi et al., 2011, Hunt et al., 2011). It has recently been reported that, on a global scale, zooplankton biomass in the whole water column increases with the average net primary production, implying an enhanced active flux of carbon coupling the surface and deep layers (Hernández-León et al., 2020).

The main objective of this study was to understand how mid-trophic level MM respond to contrasting production regimes (oligotrophic vs biologically-enriched zones) in the Kerguelen area. Specifically, we investigated the patterns and the variability of MM using a combination of stratified midwater trawl sampling and acoustic measurements. First, we tested the hypothesis that high primary production implied high abundance of MM as reported in other areas (Irigoien et al., 2014, Hernández-León et al., 2020). This response in terms of communities and densities was analysed within the Kerguelen seascape, describing the MM spatial variability. Second, the vertical pattern of variability was

examined and particularly how the vertical distribution of the various taxonomic groups differed between night and day according to the previously described communities. This knowledge on MM abundance and diel cycles according to the production and oceanographic seascape is fundamental to estimate the contribution of these organisms to the energy transfer along the food web. Finally, we assessed the vertical distribution of energy through the depth-stratified carbon content of the different taxonomic groups. Additionally, we estimated carbon flux mediated by myctophids based on family-specific physiological rates (Pakhomov et al., 1996; Belcher et al., 2019). While it was expected that productive areas also implied abundant mesopelagic fish (Irigoien et al., 2014), the contribution of these active migrators in vertical flux was assessed in HNLC *vs* productive area.

Methods

- Survey

The Mobydick survey (DOI: https://doi.org/10.17600/18000403) was carried out south of the Kerguelen Islands onboard the *R/V Marion Dufresne II*. From the 26th of February to the 19th of March 2018, hydrographic and acoustic data, as well as MM samples were collected at four stations (M1, M2, M3 and M4, Fig. 1). The comparative approach used in this study, targeting iron fertilized *vs* HNLC sites, originated from the scientific strategy of the KEOPS 1 and 2 campaigns (Queguiner et al., 2011). These stations were located based on knowledge from previous oceanographic cruises conducted in the area (e.g., Blain et al., 2007, d'Ovidio et al., 2015, Behagle et al., 2017). The M1 station was located east of the Plateau, downstream of the ACC, in the spring bloom areas known as the Keguelen plume (d'Ovidio et al. 2015), also identified as the core foraging area of the king penguin, an important top predator in terms of consuming biomass (Scheffer et al., 2016). The M2 station located on the Plateau (isobath 520 m) corresponded to a reference station to study the naturally fertilised spring bloom on the Kerguelen Plateau (Quéguiner et al. 2011). West of the Plateau, the upstream stations M3 and M4 were chosen because HNLC conditions prevailed. While M1 was visited once, M4 was visited twice and M2 thrice. The first visit of the M3 station with a full sampling of all depths during daytime and nighttime was divided into two periods because of bad weather conditions, so that M3-1 and M3-2 were separated by 11 days.

- **Remote and in-situ oceanographic measurements**

Hydrological casts were carried out at each visit of all stations (Fig. 1). Temperature (T) and chlorophyll *a* concentration (Chl *a*) profiles were collected using a SeaBird SBE 19+ Conductivity-Temperature-Depth (CTD) probe equipped with a calibrated Chelsea Aqua-Tracker Mk3 fluorometer mounted to a rosette frame holding Niskin bottles. The rosette was hauled at a speed of 1 m.s^{-1} between Niskin samples. Water collected in the Niskin bottles was used for chlorophyll a extraction and HPLC analysis as per Uitz et al. (2008). Conversion from the fluorometer measurements to Chl *a* was performed by estimating a linear fit between CTD fluorometer readings and corresponding Niskin bottle samples (n = 40, R^2 = 0.93). The mixed layer depth (MLD) was determined from the minimum depth to which $T < T_{10m} - 0.4$ °C (Condie and Dunn, 2006).

Sea surface chlorophyll data from Global Ocean Color products with a 1/24° resolution (product id: OCEANCOLOUR_GLO_CHL_L4_REP_OBSERVATIONS_009_082 from the Marine Copernicus

data portal: https://www.copernicus.eu) produced by ACRI-ST was used to build time series of Chl *a* at each station. We considered the weekly averaged L4-product (7 days) of merged satellite observations to describe the bloom temporal patterns since it represents a good compromise between the temporal resolution and the cloud coverage. We also estimated the Polar Front (PF) mean location in the Kerguelen area by using T and S profiles from the Global Ocean Reanalysis (Ferry et al., 2016), as described in Pauthenet et al. (2018).

- **Acoustic measurements**

Continuous acoustic measurements were made with a calibrated (Demer et al., 2015, Simrad EK80 documentation) Simrad EK80 echosounder operating at five frequencies, 18, 38, 70, 120 and 200 kHz. As we were interested in describing acoustic scattering in epipelagic and mesopelagic waters, we only used the 18 and 38 kHz frequencies, with maximum acquisition ranges of 1000 and 800 m respectively. Power and pulse length were respectively 2000 W and 1024 µs for 18 kHz and 1000 W and 2048 µs for 38 kHz. Data used in this study were acquired with an average ping interval of 3 s, mostly during station time when the vessel was either immobile or during trawling activity.

The acoustic data were scrutinized, corrected and analysed using the "Movies3D" software developed at the "Institut Français de Recherche pour l'Exploitation de la Mer" (Ifremer; Trenkel et al., 2009) combined with the French "Institut de Recherche pour le Développement" (IRD) open-source tool "Matecho" (Perrot et al., 2018), developed in MATLAB. The noise from the surface were removed (from 3 m below the transducer, i.e., surface 12 m removed) and the bottom ghost echoes were excluded and the bottom line was corrected. Single-ping interferences from electrical noise or other acoustic instruments (Le Bouffant, N., *comm. pers.*), and periods with either noise or attenuated signal due to inclement weather, were removed using the filters described by Ryan et al. (2015). Background noise was estimated and subtracted using methods described by De Robertis and Higginbottom (2007). The nautical area scattering coefficient (NASC in m^2 nmi^{-2}), an indicator of marine organisms' biomass, and the volume backscattering strength (Sv in dB re $1m^{-1}$), an indicator of the marine organisms' density, were calculated. Acoustic symbols and units used here follow MacLennan et al. (2002). Data were echo-integrated into 0.5 m high layers over a 3 pings period giving one ESU (Elementary Sampling Unit) with a -100 dB threshold from 12 m down to 800 m depth.

DVM is a common behaviour for zooplankton and micronekton that can be observed at almost all spatial scales (Haury et al., 1978). Acoustic data were thus split into day, night and crepuscular periods

(dawn and dusk). Day and night periods were defined based on the solar elevation angle with day when sun elevation is >18° and night with sun elevation <-18° (as in Lehodey et al., 2014).

Acoustic data were also spatially split between stations by creating a 0.8° Longitude by 0.5° Latitude rectangle around the GPS coordinate of each station (Fig. 1, blue rectangles). These rectangular areas at each station encompass the trawl operations area. Acoustic data recorded during transits (i.e., out of these spatial limits) were excluded from data analysis. The vertical profiles of mean acoustic density NASC were computed for each visit of each station for the daytime and nighttime periods (not only trawling time).

Data visualisation- Red Green Blue (RGB) composite images were generated in MATLAB based on the 18 and 38 kHz echo-integrated acoustic data as in Annasawmy et al. (2019). The acoustic volume backscattering strength Sv of the 18 kHz frequency was colour-coded in red while the 38 kHz was displayed in colder hue using both blue and green, with a high threshold scale of -60 dB and a low scale threshold of -90 dB. In the RGB composite image subsequently created, the hue gives the frequency with the highest backscatter and the luminance gives the intensity of the volume backscattering strength. A light cyan (combination of blue and green) colour indicates a dominant and high 38 kHz backscatter whereas a dark red colour indicates a dominant but low 18 kHz backscatter. A black hue indicates that all backscatters are under the low scale threshold or that no data are available, and a white hue indicates that all backscatters are above the high threshold scale. Using these two frequencies, the RGB echogram gave for each station, a clear and synthetic visual representation of the location and migration in the water column of acoustic communities of scatterers based on their most resonant frequency from 20 to 800 m.

- **Trawling**

Forty-eight trawls were performed, consisting of three nightthime trawls and three daytime trawls at each station (Table 1). MM were collected during daytime and nighttime using a Mesopelagos trawl, designed by Ifremer (fisheries biology and technology laboratory, LTBH, Lorient, France) (Meillat, 2012). This non-closing trawl has a 7 m mean vertical opening and 12 m horizontal opening, with a 65 m^2 mouth area and 44 m length. The trawl has a mesh size of 30 mm in the wings, reducing to 4 mm in the codend, so that it was used to target organisms ranging in size from approximately 1–30 cm long. Trawl depth was monitored in real-time with a Scanmar (Åsgårdstrand, Norway) depth sensor attached to the trawl headline. We adopted a semi-stratified/adaptive strategy in trawl sampling. As one aim of the study was to provide a detailed description of the micronekton community at each station, the

whole water column from the surface to 650 m was sampled at different strata corresponding to the sound scattering layers at different depths: the shallow scattering layers (SSL, between 10 and 200 m), the mid-depth scattering layers (MSL, between 200 and 500 m) and the deep scattering layers (DSL, between 500 and 800 m). At each layer, hauls were performed at targeted depths according to the observations of the different scattering structures (patches or layers) provided by the echosounders. The towing speed was maintained near 2 knots, with effective fishing times of 30 minutes. Our samples may consistently underestimate individuals smaller than the mesh size (30 mm), even slightly larger (40 mm) for micronekton with soft body such as salps. Selectivity of the mesopelagos is a shortcoming, particularly for species such as salps which can be sampled as individuals or aggregated chains. While underestimation of small individuals' may have occurred, this was consistent across all trawl deployments, i.e. across regions (Henschke et al. 2020).

Once on board, the total wet mass (WM) in grams was weighed. Organisms were first sorted into broad taxonomic groups (fish, crustaceans, gelatinous organisms and cephalopods), then identified at the species level. All organisms were counted and weighed and fish size was also measured using standard length (SL). The allocated temperature estimate for each trawl was performed by using the temperature profile from the CTD cast closest to the trawl location in space and time, and by taking the estimated temperature at the trawl depth (during the fishing period).

- Estimates of C content

Carbon biomass was estimated using conversion factors to convert WM to dry mass (DM) and DM to carbon biomass for the four main taxonomic groups - gelatinous organisms, fish, molluscs and crustaceans. Water content for each of the groups was estimated based on available data from the literature: 94% for gelatinous organisms (Larson 1986, Huntley et al 1989), 75% and 80% for fish and molluscs, respectively, (Schaafsma et al., 2018) and 75% for crustaceans (Schaafsma et al., 2018, Harris et al., 2000). The carbon content of dry biomass was provided in the context of stable isotopes analysis (Hunt et al., this issue) carried out on all the main taxa. The percentage of C in DM was then averaged for each group such as gelatinous organisms 15%, fish 50%, molluscs 35% and crustaceans 40%.

- Migrant biomass and carbon flux

Additionally, biomass and carbon flux were estimated for migratory fish of the family Myctophidae. This group was selected among others, because it exhibited a clear diel vertical migration pattern, as

described previously in this area (Duhamel et al., 2000; Behagle et al., 2017) and detected in this study through the combined trawl and acoustic data. Additionally, family-specific metabolic equations were available to predict carbon fluxes in this group (Belcher et al., 2019). On the other hand, estimations in other migratory groups were unfeasible due to sampling limitations. For example, individual body length and mass, needed for the estimation of metabolism, could not be accurately and systematically measured in salps and euphausiids, due to the deterioration of samples during trawling. We assumed that all myctophids found at nighttime in the SSL would return to MSL or DSL during daytime. Migration was then calculated as the abundance and biomass of myctophids in the nocturnal shallow trawls (ID) 5, 6, 11, 19, 20, 21, 31, 35, 37, 39, and 48 (Table 1). This was standardized for the volume filtered by the net, and it was integrated by the thickness of the sound scattering layer (from echograms) where the net was located. Abundance and biomass were expressed as the number of individuals or the milligrams of carbon weight per square metre (ind m^{-2}, mg C m^{-2}).

Carbon flux mediated by respiration was estimated by calculating the amount of carbon dioxide exhaled by myctophids below the maximum MLD in the region, which was 120 m depth. The respiration rate for each individual was estimated using body mass and environmental temperature as predictors, following the respiration regression developed for myctophid fish in Belcher et al. (2019):

$$Ln(R_{WM}) = -1.315 - 0.2665 \times Ln(WM) + 0.0848 \times T \qquad\qquad Eq.\ 1$$

where R_{WM} is the mass-specific respiration rate per hour (μl O$_2$ mg WM^{-1} h^{-1}), WM is the individual wet mass (mg), and T is the environmental temperature (^{o}C). Individual wet mass was estimated using the length-weight relationships provided for the family Myctophidae by Kwong et al. (2020). Respiration was computed for 2.2 ^{o}C, corresponding to the average temperature in waters between 400 and 500 m depth. This interval was assumed as the end of migration, according to the daytime migrant layer depth registered with the echosounder. The total respiration for each trawl was calculated by standardising the volume filtered by the net (considering a cylinder with the mouth opening of the trawl opening and the distance travelled during the haul), and summing for all myctophid individuals caught in that trawl. Similar to the abundance and biomass measurements, total respiration was integrated by the thickness of the sound scattering layer that the net sampled. This was then converted to units of carbon per square meter and day (mg C m^{-2} d^{-1}) using a respiratory quotient of 0.90 for fishes (Brett and Groves, 1979, Ariza et al., 2015) and the stoichiometric relationship between carbon and oxygen

(22.4 L O_2 = 12 g carbon). Since carbon flux to the mesopelagic zone only occurs during the daytime, only 12 hours were considered for calculations.

Carbon flux mediated by the egestion of faecal pellets, known as "gut flux", was estimated assuming that myctophids fed to satiation at the surface before migrating down to the mesopelagic zone or deeper. The food ball weight was assumed to be 2.2% of the body carbon weight, considering the average maximum stomach fullness found for southern-ocean myctophid species by Pakhomov et al. (1996). Then we assumed a 15% of loss as faeces, following conservative estimations for midwater fish from Hopkins and Baird (1977). This egestion was assumed to be constant throughout the day, so it was divided by 24 hours to compute the hourly egestion. This was multiplied by the residence time at depth (12 hours) minus the gut passage time (5.6 hours) to calculate the total carbon exported through egestion in the MSL and DSL. Gut passage time was averaged from measurements compiled for myctophid species in Pakhomov et al. (1996). Excretion of dissolved organic carbon was not computed due to the lack of knowledge about this metabolic rate in midwater fishes (Hudson et al., 2014). The amount of carbon through this mechanism is however expected to be small as dissolved matter represents a negligible part of carnivorous fish egestion, being mainly composed by non-carbon compounds such as urea and ammonia (Brett and Groves, 1979).

Carbon flux mediated by mortality at depth was estimated assuming that this was equivalent to growth, considering that the system is in a steady-state (Hernández-León et al., 2019). Growth was assumed to be 66% of respiration using metabolic budgets for carnivorous fish (Brett and Groves, 1979). Similar, to respiration and gut flux, mortality was considered only for the 12 hours residence time at depth. It is assumed that the fate of carbon transferred via predation to higher trophic levels stays in the mesopelagic zone.

Results

- Environmental conditions around the Kerguelen Plateau

In addition to their location relative to the Plateau (on the Plateau *vs* upstream/downstream areas), the stations were also situated within the area of a particular oceanographic feature, the PF, which crossed the Plateau just south of the Kerguelen Islands (Fig. 1). The M1, M2 and M4 stations were located south of the PF, with varying distances to the PF mean location, while the M3 station was located north of this front (see also Henschke et al. 2020). During the cruise, the concentration of Chl *a* was higher at station M2 on the Plateau compared to the downstream and upstream stations (Fig. 2). Overall, the Chl *a* concentrations (both over and outside the Plateau) during the survey were considered low (<0.4 mg m^{-3}) compared to the concentrations observed during the spring/summer period from October to January. Throughout this period, the highest Chl *a* was measured on the Plateau in mid-January. Medium values occurred upstream (M3 and M4) with a simultaneous peak. An earlier (late November) maximum was observed downstream.

- Description of the macrozooplancton/micronekton community from trawl collection.

Over the whole study area, the dominant biomass from obtained from the trawl samples was attributed to gelatinous organisms (Fig. 3). In most trawls, they constituted a major part of the absolute biomass, i.e. an average wet weight per sample of 6427 g (±7837 g) corresponding to a mean proportion of 63 % (±33.35 %) of the total weight (supplemental material 1). This was followed by crustaceans, with an average weight per sample of 312 g (±275 g) corresponding to a mean proportion of 30 % (±31 %), and fish with an average weight per sample of 133 g (±193 g) corresponding to a mean proportion of 6.5 % (±10.4 %).

In trawls with a low total biomass (<1000 g), crustaceans had a higher relative biomass (supplemental material 1), particularly for samples carried out during daytime at depths shallower than 300 m. This trend was supported by the high relative abundance of crustaceans, which contributed more than half of the total organisms in 75 % of the 48 trawls (supplemental material 2).

In terms of biomass, the most important gelatinous contributors were salps (S*alpa thompsoni*) followed by siphonophores (especially *Rosacea plicata*) (Fig. 4 and Table 2). Notably, *S. thompsoni* was only abundant at stations M1 and M2. Chaetognaths were also often found in trawls with relatively low biomass. Ctenophores (*Bolinopsis* sp.) and jellyfish (mostly scyphozoans) had variable contribution to the proportion of gelatinous organisms with species occurring in half of the trawls (e.g., *Calycopsis*

borchgrevinki) and contributing weakly to moderately to biomass (such as *Atolla wyvillei* and *Periphylla periphylla*).

For crustaceans, the most common species in terms of occurrence and abundance were the euphausiid *E. vallentini* and the hyperiid amphipod *Themisto gaudichaudii* (Fig. 5 and Table 3). The latter was the only species among all taxonomic groups found in all trawls, but it was particularly abundant at M2 over the shelf. The euphausiid *Euphausia triacantha* was also frequently found, though with a lower abundance than *E. vallentini*. Other hyperiid amphipods, e.g. *Cyllopus magellanicus* and *Primno macropa*, often occurred in trawls albeit at relatively low abundances

The dominant fish family was myctophid with 3367 individuals belonging to 14 species (Fig. 6 for myctophids only, Table 4 and supplemental material 1 for the main fish species). The most abundant species within the whole fish community was *Krefftichthys anderssoni*, which represents half of the fish caught when merging adults and post-larvae. *Electrona antarctica* was also an abundant species and the most frequent fish in all trawls. Other myctophids such as *Gymnoscopelus braueri* and *Protomyctophum bolini* had a high occurrence but were low to moderately abundant. Other fish families were characterized by either a high occurrence (i.e., *Notolepis coatsi* for Paralepididae) or locally a high abundance (e.g., *Bathylagus tenuis* for Bathylagidae, *Cyclothone* sp. for Gonostomatidae).

- Variability in vertical patterns from acoustic and trawl records

-Diel variability-

Diel variability in biomass and acoustic densities: A strong variability was observed in the vertical distribution of both biomass and acoustic densities between nighttime and daytime. Very low biomass was sampled in the SSL during daytime (Fig. 3). However, acoustic profiles indicated that high densities, organized in relatively thin peaks, occurred in this layer at ~100 m depth during both nighttime and daytime (Fig. 7). At depth, diel differences in biomass were less clear and acoustic densities were variable. Recurrent medium densities were observed between 400-500 m during daytime and between 250-400 m during nighttime. The 38 kHz backscatter was globally lower than the 18kHz between the surface and 500 m, while an opposite pattern occurred at depths >500 m. Although we observed (RGB echograms) diel vertical movements of acoustic structures and a patchy distribution of MM during daytime, a conspicuous 3-layers system characterized the whole area (Fig. 8). During daytime, clear scattering layers appeared and various patches, in terms of size and density, were

observed whereas acoustic layers were more scattered and consistent in the horizontal axis during nighttime. Transition periods (dusk and dawn) evidenced different patterns of vertical migrations between the surface and the underlying deeper layers, including vertical movements deeper than 800 m. Migratory organisms were more responsive at 18kHz, while a permanent non-migratory layer was observed at 600 m, which was characterized by an intense 38kHz signal (in dB).

Diel variability in communities: The most important diel variability in communities and relative biomass/abundance was observed in the SSL (i.e., above 200 m) (Fig. 3, 4, 5). The gelatinous MM (mainly salps) dominated biomass at nighttime at M1 and M2 and abundance at M1. During the night at M2, gelatinous groups and crustaceans had a similar abundance in the top 200 m layer. Crustaceans (mainly euphausiids at M1, M3 and M4 at night, Fig. 5) were lower in biomass but more abundant than gelatinous organisms. Myctophids (mainly *E. antarctica*, Fig. 6) were only present in this surface layer during nighttime. Between 200 and 500 m, gelatinous MM (mostly salps), contributed the most to total MM biomass during nighttime and a mixture with other gelatinous during daytime at M1 and M2, while siphonophores dominates the biomass in this layer at M3 and M4 (Fig. 4). Crustaceans (mainly euphausiids and hyperiids, Fig. 5) were also proportionally abundant during both periods of the day (supplemental material 2), while numerous at this depth only at M2 (Fig. 5). Fish mainly occurred in this MSL during nighttime (Fig. 6). Below 500 m (excluding the station M2), the biomass was similar for the three main taxonomic groups, in terms of both biomass and abundance, with a higher contribution of fish than in the upper layers (supplemental material 1, 2). This corresponded with higher myctophid abundance and also more bathylagids and cyclothones (supplemental material 1). Similar (relative) biomass and abundance were observed during nighttime and daytime within this DSL. Gelatinous organisms were similar to the MSL previously described, with an increased proportion of jellyfish occurring during nighttime (Fig. 4). Crustaceans presented similar biomass between nighttime and daytime.

-Inter-station variability- Lower biomass was reported for M3 and M4 stations during the nighttime in the (sub-)surface (shallower than 200 m). This main difference was mostly attributed to gelatinous organisms. While salps were abundant at M1 and M2 stations, they represented a low percentage of the gelatinous community at M3 and M4 (Table 2 and Fig. 4). The biomass at these latter stations was consequently considerably lower with a higher contribution of the other taxa, particularly siphonophores (occurring only deeper than 300m, including at M2) and to a lesser extent, ctenophores and jellyfish. Crustacean abundances between stations exhibited a different pattern. They were

numerous at the M2 station with a large proportion of the hyperiid *T. gaudichaudii* (Table 3 and Fig. 5). At other stations, euphausiids dominated the crustacean community, especially in surface waters during nighttime where large quantities were collected (at stations M1 and M4). Conversely to the crustacean pattern, the lowest abundances of fish, including the dominant myctophids, were found at M2. Despite low fish biomass at this station, a high diversity was found and *E. antarctica* was the most abundant species at all depths. At other stations, *K. anderssoni* was the dominant species, particularly in mid-depth and deeper waters during nighttime. However, *E. antarctica* was the most common species found in surface waters during nighttime and at depth during daytime. Finally, the main contrast observed in acoustic densities was reported between M2 and the other stations (Fig. 7).

-Intra-station variability- For stations visited twice (M4) or three times (M2 and M3), patterns of vertical distributions were consistent between visits, though some variability was observed. The variability was mostly observed in terms of biomass and abundance at similar depths, while the composition of the MM community was similar between visits. Acoustic profiles indicated some changes observed between visits. Densities observed during daytime at M2 decreased between the first (highest daytime biomass, Fig. 3) and the second visit. At M3 and M4, a global deepening of densities from MSL to DSL (highest fish biomass reported during the 2nd visit of M3) as well as an increase in the surface layer occurred between the first and the second visit, especially during nighttime.

- Carbon content in each taxonomic group

Due to low carbon content, the contribution of gelatinous plankton to total carbon biomass was important but decreased significantly in comparison with their contribution to wet biomass (average of 29.85 % (±25.46 %) for gelatinous, 51.69 % (±31.04 %) for crustaceans and 18.88 % (±23.51 %) for fish, Fig. 9). At most of the stations (M1, M3 and M4), fish dominated carbon biomass in the DSL (average of 38.37 % (±26.37 %)), especially for the night trawls (average of 50.54 % (±22.49 %)). In surface layers, crustaceans were usually the major contributors to carbon biomass, except for a few stations where gelatinous organisms were dominant (Fig. 9).

- Carbon flux

The abundance, biomass, and carbon flux from myctophids entering the MSL and the DSL during daytime ranged from 0.001 to 0.163 ind m^{-2}, from 0.04 to 15.08 mg C m^{-2}, and from 0.001 to 0.091 mg C m^{-2} d^{-1}, respectively. According to Fig. 10, the downstream and upstream stations off the Plateau (respectively M1 and M4), exhibited the highest values of abundance, biomass, and carbon export,

while stations over and close to the Plateau (respectively M2 and M3) had the lowest values. Averaged Chl a, from 20 to 100 m depth, ranged from 0.19 to 0.60 mg m^{-3} during the visits where carbon fluxes were estimated (Fig. 10a-b). As a result of the varying hydrographic conditions (MLD for instance) found at each visit, the distribution of migratory scattering layers changed as observed on echograms, and the depth range of trawling was adjusted to target these layers (e-h). The highest values on abundance, biomass, and carbon flux coincided with intermediate Chl a values in M1 and M4, in migratory layers sampled between 21 and 96 m depth (trawls 11, 21, 31 in Fig. 10), while the lowest values coincided with the Chl a maxima at M2, in migratory layers sampled between 21 and 175 m (trawls 37, 39 in Fig. 10). Carbon flux was fundamentally driven by biomass, which was in turn driven by the total number of individuals in the catch. This resulted from the overall similar size distributions between trawls, with individuals mostly ranging from 10 to 70 mm standard length (see supplementary material 2). Exceptionally, in trawls 6 and 20 at station M2, the occurrence of a few individuals larger than 100 mm increased the total biomass but decreased carbon flux as a result of lower metabolic rates of large fish (see equation 1). It is worthy to note that these two trawls were carried out in the SSL, but below the MLD.

Discussion

The waters surrounding the Kerguelen Islands encompassed variable communities of macrozooplankton-micronekton (MM), with respect to their biomasses, proportional contributions, and vertical patterns. Because vertical active fluxes are generally driven by biomass and composition, this has important implications for the regional and global biological pump (Ariza et al., 2015, Gorgues et al., 2019, Hernández-León et al., 2019). This study revealed the MM variability in response to the particular physical features and biological characteristics of this dynamic area.

1. Macrozooplankton-micronekton communities within the Kerguelen seascape

Our results provide a detailed description of the MM communities following a longitudinal gradient across the Kerguelen Plateau, and serves as a case study of an area of the Southern Ocean where contrasting production regions occur. As expected, the MM communities varied according to these environments differing in terms of bathymetry, downstream vs upstream location relative to the Plateau, level of Chl *a* and position relative to the PF (north vs south)

Over the Plateau area and south of the PF (M3), the MM community was rich in terms of abundance and biomass, especially for salps and crustaceans (*T. gaudichaudii*, as previously reportedby Carlotti et al.(2015), and to a lower extent *E. vallentini*) Fish were less abundant but species diversity is higher compared to the other areas. While Chl *a* was relatively low during the sampling period, it had been preceded by a strong bloom. Indeed, this area is characterized by a reoccurring large phytoplankton bloom induced by naturally iron fertilized waters from the Plateau (Blain et al., 2007). Sustained blooms as observed on the Plateau station favour a high secondary production rate and a general increase in zooplankton herbivory, as observed during the KEOPS2 survey (Carlotti et al., 2015). Low advection and high residence time occurring over the Plateau also support the hypothesis of local transfer of biomass through the trophic web (Henschke et al. 2015).

In the downstream area corresponding to the Kerguelen plume south of the PF (M1), salps largely dominated the biomass. Euphausiids (mainly *E. vallentini*) and fish (*K. anderssoni* and *E. antarctica)* were abundant in different layers according to their diel cycle (Duhamel et al. 2000 for fish DVM). Here the Chl *a* biomass peaked three months earlier and was low during the cruise. This area is considered highly dynamic with low residence time at local scale. However, it is located in the downstream recirculation area of the large PF meander as described in d'Ovidio et al. (2015)

supporting the development of a rich food web in this mesoscale retentive feature. As an indicator of high MM abundance and accessibility (Béhagle et al., 2017), the eastern slope of the Kerguelen Plateau is a well-known foraging area for top predators such as king penguins (*Aptenodytes patagonicus*), macaroni penguins (*Eudyptes chrysolophus*) and fur seals (*Arctocephalus gazella*), which predominantly forage within the SSL on crustaceans and myctophids (Bost et al., 2002, Lea and Dubroca 2003, Sato et al., 2004).

As hypothesized, low overall MM biomasses were reported in the low-chlorophyll upstream area, mainly due to low salp densities. West of the Plateau and south of the PF (M4), siphonophores dominated the total biomass while migrating euphausiids and myctophids (*K. anderssoni* and *E. antarctica*) were found in high densities in the SSL and jellyfish were significant in the deeper layers. The lowest overall biomass was found at the previous HNLC KERFIX station (Jeandel et al. 1998), located closer to the Plateau and north of the PF (M3). Here, gelatinous group (siphonophores, jellyfish and ctenophores) and fish (bathylagids and *Cyclothone* sp) exhibited a high diversity, crustacean abundance was low and fish also made a relatively high contribution to biomass. This particular community corresponded to warmer waters north of the PF delimiting the northern extent of the distribution area of the endemic Antarctic species *E. antarctica* (Duhamel et al., 2014). Upstream of the Plateau, the PF location is highly variable and undergoes a large seasonal change (Pauthenet et al., 2018). These authors reported that the PF is located at its southernmost position in March, i.e., during the survey period. As a consequence, the location of station M3 in relation to the PF may have shifted in the previous months and resulted in different physical and biogeochemical conditions. Moreover, the purported HNLC upstream area (especially at M4) presented similar levels of Chl *a* than the downstream M1 station. The spring-summer production at upstream stations was abnormally high when compared to the averaged Chl *a* in this area (Christaki et al., 2021), potentially influencing the densities of the MM populations and maybe partly blurring the effect of contrasting production regimes.

2. Diel cycles and intra-station variability as sources of time varying patterns
Despite clear differences in the vertical distribution of both acoustic densities and biomass-abundance between daytime and nighttime, a consistent three-layer system occurred over the whole study area from upstream to downstream regions of the Plateau. While higher total biomass was observed during nighttime, particularly in the surface layer, acoustic densities were remarkably similar between daytime and nighttime. This acoustic peculiarity was especially noticeable in the SSL where various densities

were reported at the two frequencies. Here, very few gelatinous organisms and fish were collected, and crustaceans dominated trawls during daytime. The combination of trawl avoidance during daylight and diurnal behaviour of myctophids could explain why their biomass were undersampled in the surface layer (Kaartvedt et al., 2012). Indeed, fish schooling is a diurnal behaviour leading to a patchy distribution during the day that vanishes at night (Saunders et al., 2013). The peak in acoustic densities above 100 m during daytime at both frequencies (particularly at 18 kHz) likely corresponded to a thin layer where small schools of myctophids occurred. This is supported by both previous acoustic measurements carried out in the area east of the Plateau corresponding to the station M1 (Behagle et al., 2017), and the diving depth of king penguins that feed mostly on *K. anderssoni* during daytime (Scheffer et al., 2016). Few fish species were caught in SSL during the day, with the shallow acoustic densities being likely *K. anderssoni* (Duhamel et al., 2000; Hunt and Swalding, 2021). The vertical distribution of this non-migratory species is based on age-segregation: juveniles are intensively feeding in the warm and productive surface waters while adults were found deeper (Lourenço et al., 2017).

The diel cycle in the SSL was the largest contrast we observed, with the invasion of gelatinous, crustaceans and mesopelagic fish from mid- and deep layers to the epipelagic. The daily difference in biomass and in the RGB echograms evidenced the migratory pattern of numerous species, including *i)* salps, which were found deeper than 200 m in the morning and performed a first migration to subsurface at mid-day, before moving up to the surface layer at night (Nishikawa and Tsuda 2001, Henscke et al., 2021); *ii)* the main crustacean species, i.e. *E. vallentini* that performed DVM from subsurface-deep waters (100 m to 300 m depth) during daytime to the surface layer during nighttime (Mauchline and Fisher, 1969, Boden and Parker, 1986), and *T. gaudichaudii* that also displayed DVM through a more complex pattern due to an ontogenetic component, with juveniles moving in the upper 100 m whereas adults descended to depths below 200 m during daytime (Pakhomov and Froneman, 1999); and *iii)* the myctophid *E. antarctica* exhibited a typical DVM, occurring within the surface waters during the night and descending below 300 m during daytime, with a size component (larger individuals found deeper than 600 m at night, while small fish were located at 300-400 m during the day; Hulley and Duhamel, 2011). Other important contributors were non- or slightly migratory species, such as *K. anderssoni* (see above) and the siphonophore *R. plicata* that exhibited a quasi-permanent distribution below 300 m with minor diel movements (as suggested in Pugh 1984).

Multiple layers and patches and diverse DVMs during the transition periods were observed on the RGB echograms. This bi-frequency visualization was particularly insightful to understand the vertical

patterns of averaged acoustic profiles that appeared relatively similar during both day and night periods. Here, we attempted to interpret this three-layer system based on the combination of bi-frequency responses and trawl sampling obtained during our survey and on the already known diel vertical distribution. During daytime, SSL was dominated by juveniles of *K. anderssoni* and of *T. gaudichaudii*, while this layer was invaded by numerous species at night from deeper waters, including salps, fish *E. antarctica*, and euphausiid *E. vallentini*. Preliminary results using the four-frequency comparison (but limited to the surface layer) indicated a more complex pattern with layers presenting multi-acoustic responses indicative of multi-species structures. During daytime, salps distributed in the upper part (~200 m) of MDL in the morning (patch observed on the RGB echogram in the downstream area), before moving up at mid-day, as indicated by a strong response at 18kHz (Wiebe et al., 2010). A mix of the main crustacean species (*E. vallentini* and adults *T. gaudichaudii* between 200 m and 300 m) was found on the Plateau. The lower part of the MDL was attributed to siphonophores collected below 300 m, combined with crustaceans. During nighttime, crustaceans mainly migrated to the SSL, while siphonophores constituted a permanent layer below 300 m, moving slightly upward at night. Over the plateau, waters just above the bottom were characterized by a permanent layer that was found deeper (~600 m) at the other stations. During daytime in the DSL, this permanent 38kHz-dominated layer, centred at 600 m, was probably characterized by the main fish species in the area, i.e., large specimens of *E. antarctica*, adults of *K. anderssoni*, bathylagids and *Cyclothone* sp., together with siphonophores and euphausiids. During the night, a part of this fish community, probably juveniles or the smallest individuals, move upward together with euphausiids. However, a 600 m-depth layer remained permanently, with the same combination of organisms that was acoustically dominated by fish. The higher 38kHz acoustic levels compared to the 18kHz at the DSL could be due to this fish dominance, since larger non-migrant *E. antarctica* individuals have a reduced gaseous swimbladder relative to the smaller individuals that have a large air-filled swimbladder (Dornan et al. 2019). Other acoustic layers occurred deeper, at the limit of the 38kHz vertical range, where just two trawls were carried out, and reported a similar community with more deep-sea species such as jellyfish.

The vertical patterns in biomass and communities together with the diel cycles were consistent between visits on the Plateau and in the upstream area. It suggested that the same MM populations were sampled at each station where a low horizontal transport occurred (Henschke et al., 2021). The occasional variability in biomass and abundance in the same layers could indeed be attributed either to the known MM patchiness (i.e., spatial variability) or to the development of trophic interactions (i.e., temporal variability).

While the combination of trawl and acoustic sampling clearly benefited the description of the MM community, it is crucial to bear in mind the specificities of each methodology (Ariza et al., 2016). Despite the possibility of contamination of deep hauls by upper organisms due to the use of a non-closing trawl, we reduced this effect through fast launch and haul out during trawl operations. Moreover, while numerous species' were sampled, we only focused on the most abundant species. This precaution was particularly suitable in our study area where the dominant species were limited and represented a very high proportion of biomass and abundance, consequently contributing significantly to the backscatter. In turn, acoustic measurements were based on the properties of the dominant species in a volume containing many organisms, either in terms of relative backscatter intensity dominated by the strongest reflector or due to the frequency-dependent response. This implies that gas-bearing organisms, such as fish with air-filled swimbladders or siphonophores, dominated small fluid-like organisms at 18kHz and 38kHz (Ariza et al., 2016, Behagle et al., 2017).

3. Variability in vertical distribution of carbon content and active flux associated with macrozooplankton-micronekton.

Although gelatinous groups dominated the wet biomass in the majority of trawls, organism energy content needs to be taken into account with respect to sustaining the development of higher trophic levels. For example, crustaceans are higher quality food than gelatinous organisms, such as salps (Harmelin-Vivien et al., 2019). Considering carbon content allows a better estimate of the relative contribution of the different groups in terms of their roles in the energy transfer along the food web. Mesopelagic fish represented the main source of carbon stock in the DSL. They were shown to play an important role in active transfer of carbon from the surface-intermediate layers to deep waters (Belcher et al., 2019). The extent of the active carbon flux driven by fish depends on the species composition, with not all species performing DVM (Romero-Romero et al., 2019, Klevjer et al., 2020). In our study, some of the highest fish carbon biomasses were measured at station M3, where relatively low abundances of crustacean were found in the upper layer (including zooplankton, see Hunt et al., this issue), potentially implying some top down control. However, primary productivity in surface waters at this upstream station was low, which may have contributed to the low crustacean biomass, and further, it is questionable whether such low biomass of fish can impact crustacean abundance (Pepin et al., 2013). Crustacean and gelatinous organisms represented a large, although varying, C stock on the Plateau, but they were not associated with high mesopelagic fish biomass, possibly due to depth

limitation (550 m depth over the shelf). For consistency, we used an average of water carbon content computed for each of the groups, based on available data from the literature. However, we acknowledge that variability can be observed between species of the groups and between different estimates within the same species. Such variability can be explained by the different geographic areas where the same species occurred and the samples obtained at different seasons, both potentially affecting the body composition of organisms (Schaafsma et al., 2018).

Additionally, we estimated the carbon flux mediated by migratory fish from the myctophid family, a major component in the Southern Ocean food web (Pakhomov et al., 1996; Saunders et al., 2019) and known to play an important role in the active transport of carbon to the deep ocean (Davison et al., 2013; Ariza et al., 2015; Belcher et al., 2019; Kwong et al., 2020). Due to sampling constraints and level of knowledge (see methods), myctophids were the group selected to estimate carbon over salps, euphausiids, or hyperiids, which represented higher biomass at least according to the net trawling results (Fig. 3-8). Without discrediting the important role of the latter groups in the subantarctic food webs (Perissinoto et al., 1998; Pakhomov et al., 2002), it should be considered that our biomass data might be strongly affected by the catchability and selectivity performance of our trawling net (Meillat, 2012, Béhagle et al., 2017). Myctophids are fast swimmers and they are expected to efficiently avoid trawling nets (Kaartvedt et al., 2012), especially when compared to quasi-drifting life forms like salps, or to smaller organisms such as euphausiids or hyperiids (Skjoldal, et al. 2013). Trawl avoidance can make a difference, considering that we used a net with a 65 m^2 mouth area. Hence, we presumed that myctophids were undersampled and are an important component of the DVM in the region, according to literature (Pakhomov et al., 1996; Saunders et al., 2019). This, along with the extraordinary migration extent of organisms, often beyond 700-800 m depth when they are larger than 40 mm (Badcock and Merret, 1976), made pertinent the estimation of carbon flux on this group. Interestingly, larger fish were sampled below the MLD over the Plateau. While they did not perform inter-zonal migration, they nonetheless contribute at a lower extent to the downward carbon flux as the acoustic backscatter during nighttime at this depth was not observed during daytime due to fish downward migration from SSL to deeper layers.

Our carbon flux estimation strongly relies on individual body mass and environmental temperature, using a respiration rate predictive equation (see methods). As discussed by Belcher et al. (2019), species-specific metabolism variance is not accounted for by this predictive equation and this should be added, along with the capture efficiency of the net, as factors potentially influencing our results.

Capture efficiency and metabolic models are a common source of uncertainty to estimate carbon flux in micronekton, and this might explain why results generated over the last two decades still differ by up to three orders of magnitude (see Table 5). Our respiratory carbon flux estimations, ranging from 0.001 to 0.045 mg C m^{-2} d^{-1}, are for instance one order or magnitude lower than those obtained by Belcher et al. (2019) in the Atlantic sector of the Southern Ocean, using the same predictive equation, and based on non-corrected catch data, as we did (see Table 5). This demonstrates the urgent need to perform further inter-calibration experiments on micronekton samplers and acoustics (Pakhomov et al., 2010, Kaartvedt et al., 2012), and to work towards obtaining more accurate metabolic models for species involved in DVM (Belcher et al., 2019, 2020). In this study, the mesopelagos net is known to strongly undersample large fish (Meillat, 2012, Béhagle et al., 2017). Respiration is also expected to be underestimated in cold temperature environments, because the predictive equation was partially built from respiration rates calculated for temperate and tropical species (Belcher et al., 2020). Our active carbon flux values might therefore be underestimated to an unknown degree, and until these uncertainties are resolved, the results should be interpreted with caution in absolute terms. Indeed, the most recent inter-comparison of carbon fluxes between epi- and mesopelagic zones using a linear inverse ecosystem model suggested that estimates of zooplankton active transport using conservative estimates of standard metabolism are grossly underestimated (Kelly et al. 2020). Relative values among stations and visits were however revealing about how environmental factors and population dynamics can affect carbon flux. For instance, Figure 10 illustrates how carbon flux is strongly driven by the total migrant biomass, but that this biomass will be more efficiently converted into exported carbon when the size structure of the community is small. This results from higher metabolic rates for small fish (Equation 1). On the other hand, the migration range in small myctophid fishes smaller and shallower (Badcock and Merrett, 1976), with significant implications when modelling fish-mediated carbon flux. Overall, the ocean-basin and slope-boundary stations M1 and M4, situated south off the PF, had greater migrant biomass, larger species, and twofold to threefold higher respiratory carbon fluxes. This highlights the importance of patchiness and community composition when assessing carbon flux, and demonstrate a strong bottom up structuring on the active component of the biological pump.

Conclusion

The complementary collection of trawl and acoustic data contribute to elucidate MM diversity, its complex horizontal and vertical organisation and the associated biogeochemical fluxes in the different primary production regimes in the Kerguelen region. While a consistent three-layers system has been determined between 12 m and 800 m over the Kerguelen seascape, the MM assemblage defined the

vertical patterns and its associated DVM. As expected, the highest biomasses of MM were found in productive areas on the Plateau and downstream. However, carbon content and flux from migrating myctophids, which contributed significantly to the carbon MM biomass, did not follow the same pattern. In order to obtain reliable active transport estimates of the different MM taxonomic groups, which are likely slightly to substantially underestimated, a comprehensive sampling effort should be deployed using multiple techniques: net samplings, acoustics, video imaging and genetics. The aim of this effort would be twofold, clarification of ecological diversity and biogeochemical basis of these organisms or ground truthing standing stocks for their sustainable management. The biophysical links also deserve urgent attention to enable describing the influence of physical features, such as the water mass stratification, the PF position at the Plateau and offshore areas, on pelagic food webs.

Acknowledgements

Declaration of interests

The authors declare that they have no known competing financial interests or personal relationships that could have appeared to influence the work reported in this paper.

References

Anderson, T.R., Martin, A.P., Lampitt, R.S., Trueman, C.N., Henson, S.A., Mayor, D.J., 2018. Quantifying carbon fluxes from primary production to mesopelagic fish using a simple food web model. ICES J. Mar. Sci. 76, 690–701. https://doi.org/10.1093/ icesjms/ fsx234

Annasawmy, P., Ternon, J.-F., Cotel, P., Cherel, Y., Romanov, E.V., Roudaut, G., Lebourges Dhaussy, A., Ménard, F., Marsac, F. 2019. Micronekton distributions and assemblages at two shallow seamounts of the south-western Indian Ocean : insights from acoustics and mesopelagic trawl data. Prog. Oceanogr. 178, art. 102161.

Ariza, A., Garijo, J.C., Landeira, J.M., Bordes, F., Hernández-León, S., 2015. Migrant biomass and respiratory carbon flux by zooplankton and micronekton in the subtropical northeast Atlantic Ocean (Canary Islands). Prog. Oceanogr. 134, 330–342.

Ariza, A., Landeira, J. M., Escánez, A., Wienerroither, R., Aguilarde Soto, N., Røstad, A., Kaartvedt, S., and Hernández-León,S. 2016. Vertical distribution, composition and migratory patterns of acoustic scattering layers in the Canary Islands, J. Mar. Syst.,157, 82–91. https://doi.org/10.1016/j.jmarsys.2016.01.004,2016.

Badcock, J., Merrett, N.R., 1976. Midwater fishes in the eastern North Atlantic–I. Vertical distribution and associated biology in 30N, 23W, with developmental notes on certain myctophids. Prog. Oceanogr. 7, 3–58.

Béhagle, N., Cotté, C., Lebourges-Dhaussy, A., Roudaut, G., Duhamel, G., Brehmer, P., Josse, E., Cherel, Y., 2017. Acoustic distribution of discriminated micronektonic organisms from a bi-frequency processing: The case study of eastern Kerguelen oceanic waters. Prog. Oceanogr. 156, 276-289.

Behrenfeld, M.J., Gaube, P., Della Penna, A. et al., 2019. Global satellite-observed daily vertical migrations of ocean animals. Nature 576, 257–261. https://doi.org/10.1038/s41586-019-1796-9

Belcher, A., Cook, K., Bondyale-Juez, D., Stowasser, G., Fielding, S., Saunders, R.A., Mayor, D.J., Tarling, G.A., 2020. Respiration of mesopelagic fish: a comparison of respiratory electron transport system (ETS) measurements and allometrically calculated rates in the Southern Ocean and Benguela Current. ICES J. Mar. Sci. fsaa031.

Bianchi, D., Stock, C., Galbraith, E. D., Sarmiento, J. L., 2013. Diel vertical migration: Ecological controls and impacts on the biological pump in a one-dimensional ocean model. Global Biogeochem. Cycles 27, 478–491. https://doi:10.1002/gbc.20031

Blain, S., et al.,2007. Effect of natural iron fertilization on carbon sequestration in the Southern Ocean. Nature 446, 1070–1074. https://doi:10.1038/nature05700.

Bocher, P., Cherel, Y., Labat, J.P., Mayzaud, P., Razouls, S., Jouventin, P., 2001. Amphipod-based food web: *Themisto gaudichaudii* caught in nets and by seabirds in Kerguelen waters, southern Indian Ocean. Mar. Ecol. Prog. Ser. 223, 261–276.

Boden, B. P., Parker, L. D., 1986. The plankton of the Prince Edward Islands. Polar Biol. 5, 81–93.

Bost, C., Zorn, T., Le Maho, Y., Duhamel, G., 2002. Feeding of diving predators and diel vertical migration of prey: King penguin's diet versus trawl sampling at Kerguelen Islands Mar. Ecol. Prog. Ser. 227, 51–61.

Brett, J.R., 1979. Factors affecting fish growth, in Fish Physiology Volume 8 (eds W.S. Hoar, D.J. Randall and J.R. Brett), Academic Press, New York, pp. 599–675.

Brett, J.R.,Groves, T.D.D., 1979. Physiological energetics, in Fish Physiology Volume 8 (eds W.S. Hoar, D.J. Randall and J.R. Brett), Academic Press, New York, pp. 279–281.

Carlotti, F., Jouandet, M.-P., Nowaczyk, A., Harmelin-Vivien, M., Lefèvre, D., Richard, P., Zhu, Y., Zhou, M.,2015) Mesozooplankton structure and functioning during the onset of the Kerguelen phytoplankton bloom during the KEOPS2 survey, Biogeosciences 12, 4543–4563, https://doi.org/10.5194/bg-12-4543-2015.

Cherel ,Y., Bocher, P., de Broyer, C., Hobson, K.A., 2002. Food and feeding ecology of the sympatric thin-billed *Pachyptila belcheri* and Antarctic P. desolata prions at Iles Kerguelen, Southern Indian Ocean. Mar. Ecol. Prog. Ser. 228, 263-281.

Cherel, Y., Ducatez, S., Fontaine, C., Richard, P., Guinet, C., 2008. Stable isotopes reveal the trophic position and mesopelagic fish diet of female southern elephant seals breeding on the Kerguelen Islands. Mar. Ecol. Prog. Ser. 370, 239-247.

Christaki, U., Gueneugues, A., Liu, Y., Blain, S., Catala, P., Colombet, J., Debeljak, P., Jardillier, L., Irion, S., Planchon, F., Sassenhagen, I., Sime-Ngando, T., Obernosterer, I., 2021. Seasonal microbial food web dynamics in contrasting Southern Ocean productivity regimes. Limnol. and Oceanogr. 66,108-122.

Condie, S.A., Dunn, J.R., 2006. Seasonal characteristics of the surface mixed layer in the Australasian region: implications for primary production regime and biogeography. Mar. Freshw. Res. 57, 569–590.

de Baar, H.J.W., de Jong, J.T.M., Bakker, D.C.E., Löscher, B.M. , Veth, C. , Bathmann, U., Smetacek, V., 1995. Importance of iron for phytoplankton spring blooms and CO2 drawdown in the Southern Ocean. Nature 373, 412–415.

De Robertis, A., Higginbottom, I., 2007. A post-processing technique to estimate the signal-to-noise ratio and remove echosounder background noise. ICES J. Mar. Sci. 64, 1282–1291.

d'Ovidio, F., Della Penna, A., Trull, T. W., Nencioli, F., Pujol, M.-I., Rio, M.-H., Park, Y.-H., Cotté, C., Zhou, M., Blain, S., 2015. The biogeochemical structuring role of horizontal stirring: Lagrangian perspectives on iron delivery downstream of the Kerguelen Plateau. Biogeosciences 12, 5567–5581. https://doi.org/10.5194/bg-12-5567-2015

Davison, P.C., Checkley, D.M., Koslow, J.A., Barlow, J., 2013. Carbon export mediated by mesopelagic fishes in the northeast Pacific Ocean. Prog. Oceanogr. 116, 14–30.

Demer, D.A., Berger, L., Bernasconi, M., Bethke, E., Boswell, K., Chu, D., Domokos, R., et al. 2015. Calibration of acoustic instruments. ICES Cooperative Research Report No. 326. 133 pp. https://doi.org/10.17895/ices.pub.5494

Dornan, T., Fielding, S., Saunders, R.A., Genner, M.J., 2019. Swimbladder morphology masks Southern Ocean mesopelagic fish biomass. Proc. R. Soc. B. 286, 20190353. http://doi.org/10.1098/rspb.2019.0353

Duhamel, G., Koubbi, P., Ravier, C., 2000. Day and night mesopelagic fish assemblages off the Kerguelen Islands (Southern Ocean). Polar Biol. 23, 106–112.

Duhamel, G., Hulley, P.A., Causse, R., Koubbi, P., Vacchi, M., Pruvost, P., Vigetta, S., Irisson, J.O., Mormède, S., Belchier, M., Dettai, A., Detrich, H.W., Gutt, J., Jones, C.D., Kock, K.H., Lopez Abellan, L.J., Van de Putte, A.P., 2014. Biogeographic patterns of fish. Biogeographic Atlas of the Southern Ocean, 7, 328-362.

Gorgues, T., Aumont, O., Memery, L., 2019. Simulated changes in theparticulate carbon export efficiency due to diel vertical migration ofzooplankton in the North Atlantic. Geophys. Res. Lett. 46, 5387–5395. https://doi.org/10.1029/2018GL08174

Grimaldo, E., Grimsmo, L., Alvarez, P., Herrmann, B., Tveit, G.M., Tiller, R., Slizyte, R., Aldanondo, N., Guldberg, T., Toldnes, B., et al., 2020. Investigating the potential for a commercial fishery in the Northeast Atlantic utilizing mesopelagic species. ICES J. Mar. Sci. 77,2541–2556. doi: 10.1093/icesjms/fsaa114

Guinet, C., Cherel, Y., Ridoux, V., Jouventin, P., 1996. Consumption of marine resources by seabirds and seals in Crozet and Kerguelen waters: changes in relation to consumer biomass 1962-85. Antarct. Sci. 8, 23-30.

Harmelin-Vivien, M., Bănaru, D., Dromard, C. R., Ourgaud, M., Carlotti, F., 2019. Biochemical composition and energy content of size-fractionated zooplankton east of the Kerguelen Islands. Polar Biol. 42, 603-617. doi:10.1007/s00300-019-02458-8

Harris, R.P., Wiebe, P., Lenz, J., Skjoldal, H.R., Huntley, M., 2000. Zooplankton Methodology Manual, Academic, London, U.K.

Haury, L.R., McGowan, J.A., Wiebe, P.H., 1978. Patterns and processes in the time-space scales of plankton distributions. In: Steele JH, editors. Spatial patterns inplankton communities. Plenum Press, New York. 277–327.

Henschke, N., Blain, S., Cherel, Y., Cotté, C., Espinasse, B., Hunt, B.P.V., Pakhomov, E.A., 2021. Population demographics and growth rate of *Salpa thompsoni* on the Kerguelen Plateau. J. Mar. Syst. 214, 103489.

Hernández-León, S., Olivar, M. P., Luz, M., De Puelles, F., Bode, A., Castellón, A., López-pérez, C. et al., 2019. Zooplankton and micronekton active flux across the tropical and subtropical Atlantic Ocean. Front. Mar. Sci. 6, 1–20.

Hernández-León, S., Koppelmann, R., Fraile-Nuez, E. et al., 2020. Large deep-sea zooplankton biomass mirrors primary production in the global ocean. Nat. Commun. 11, 6048. https://doi.org/10.1038/s41467-020-19875-7

Hindell, M.A., Lea, M.-A., Bost, C.A., Charrassin, J.-B., Gales, N., Goldsworthy, S.D., Page, B., Robertson, G., Wienecke, B., O'Toole, M., Guinet, C., 2011. Foraging habitats of top predators, and areas of ecological significance, on the Kerguelen Plateau. In: Duhamel, G., Welsford, D.C. (Eds.), The Kerguelen Plateau: Marine Ecosystem and Fisheries. Société Française d'Ichtyologie, Paris, 203–215.

Hopkins, T.L., Baird, R.C., 1977. Aspects of the feeding ecology of oceanic midwater fishes. In: Oceanic sound scattering prediction, pp 325–360. Ed. by W. R. Anderson and B. J. Zahuranec. New York: Plenum Press

Hudson, J., Steinberg, D., Sutton, T., Graves, J., Latour, R., 2014. Myctophid Feeding Ecology and Carbon Transport Along the Northern Mid-Atlantic Ridge. Deep Sea Res. Part I. 93, 104-116

Hulley, P.A., Duhamel., G., 2011. Aspects of lanternfish distribution in the Kerguelen Plateau region. In: G. Duhamel and D.C. Welsford (Eds). The Kerguelen Plateau: marine ecosys-tems and fisheries. Société Française d'Ichthyo-logie, Paris, 183–195

Hunt, B.P.V., Pakhomov, E.A., Williams, R., 2011. Comparative analysis of the 1980s and 2004 macrozooplankton composition and distribution in the vicinity of Kerguelen and Heard Islands: seasonal cycles and oceanographic forcing of long-term change. In: Duhamel, G., Welsford, D. (Eds.), The Kerguelen Plateau: Marine Ecosystem and Fisheries. Société Française d'Ichtyologie, Paris, 79–92.

Hunt, B.P.V., Swadling, K.M., 2021. Macrozooplankton and micronekton community structure and diel vertical migration in the Heard Island Region, Central Kerguelen Plateau. J. Mar. Syst. 221:103575. https://doi.org/10.1016/j.jmarsys.2021.103575

Hunt, B.P.V., Espinasse, B., Henschke ,N., Cherel, Y., Cotté, C., Delegrange, A., Pakhomov, E.A., Planchon F. Trophic pathways and transfer efficiency from phytoplankton to micronekton under contrasting productivity regimes in the Kerguelen Islands region, Southern Ocean. This issue

Huntley, M.E., Sykes, P.F., Marin, V., 1989. Biometry and trophody-namics of *Salpa thompsoni* Foxton (Tunicata, Thaliacea) near the Antarctic Peninsula in austral summer, 1983–1984. Polar Biol. 10, 59–70.

Irigoien, X., Klevjer, T. A., Røstad, A., Martinez, U., Boyra, G., Acuña, J. L., et al., 2014. Large mesopelagic fishes biomass and trophic efficiency in the open ocean. Nat. Commun. 5, 3271. doi:10.1038/ncomms4271

Jeandel, C., Ruiz-Pino, D., Gjata, E., Poisson, A., Brunet, C., Charriaud, E., Dehairs. F., Delille, D., Fiala, M., Fravalo, C., Miquel, Jc., Park, Hy., Pondaven, P., Queguiner, B., Razouls, S., Shauer, B., Treguer, P., 1998. KERFIX, a time-series station in the Southern Ocean: a presentation. J. Mar. Syst. 17, 555-569. https://doi.org/10.1016/S0924-7963(98)00064-5

Kaartvedt, S., Staby, A., Aksnes, D.L., 2012. Efficient trawl avoidance by mesopelagic fishes causes large underestimation of their biomass. Mar. Ecol. Prog. Ser. 456,1-6. https://doi.org/10.3354/meps09785

Kelly. T.B., Davison, P.C., Goericke, R., Landry, M.R., Ohman, M.D., Stukel, M.R., 2019. The importance of mesozooplankton diel vertical migration for sustaining a mesopelagic food web. Front. Mar. Sci. 6,508. doi: 10.3389/fmars.2019.00508

Klevjer, T.A., Melle, W., Knutsen, T., Aksnes, D.L., 2020. Vertical distribution and migration of mesopelagic scatterers in four north Atlantic basins. Deep Sea Res. Part II. 104811. https://doi.org/10.1016/j.dsr2.2020.104811

Koubbi, P., Hulley, P.A., Raymond B., Penot, F., Gasparini, S., Labat, J.-P., Pruvost P., Mormède, S., Irisson, J.O., Duhamel, G., Mayzaud, P., 2011. Estimating the biodiversity of the sub-Antarctic Indian part for ecoregionalisation: Part I. Pelagic realm of CCAMLR areas 58.5.1 and 58.6. CCAMLR. WS-MPA-11/11, 1-39.

Kwong, L.E., Henschke, N., Pakhomov, E.A., Everett, J.D., Suthers, I.M., 2020. Mesozooplankton and Micronekton Active Carbon Transport in Contrasting Eddies. Front. Mar. Sci. 6, 825. doi: 10.3389/fmars.2019.00825

Le Moigne, F.A.C., et al., 2016. What causes the inverse relationship between primary production and export efficiency in the Southern Ocean? Geophys. Res. Lett. 43, 4457–4466. doi:10.1002/2016GL068480

Larson, R.J., 1986. Water content, organic content and carbon and nitrogen composition of medusae from the northeast Pacific. J. Exp. Mar. Biol. Ecol. 99, 107-120.

Lea, M.A., Cherel, Y., Guinet, C., Nichols, P.D., 2002. Antarctic fur seals foraging in the Polar Frontal Zone: inter-annual shifts in diet as shown from fecal and fatty acid analyses. Mar. Ecol. Prog. Ser. 245, 281-297. [Erratum in Mar Ecol Prog Ser 253:310, 2003]

Lehodey, P., Conchon, A., Senina, I., Domokos, R., Calmettes, B., Jouanno, J., Hernández, O., Kloser, R., 2014. Optimization of a micronekton model with acoustic data. ICES J. Mar. Sci. 72, 1399–1412.

Longhurst, A.R., 1976. Vertical migration in The Ecology of the Seas,D. H. Cushing and J. J. Walsh, Blackwell Science, London, pp. 116–137.

Lourenço S., Saunders R.A., Collins M., Shreeve R., Assis C.A., Belchier M., Watkins J.L., Xavier J.C., 2017. Life cycle, distribution and trophodynamics of the lanternfish *Krefftichthys anderssoni* (Lönnberg, 1905) in the Scotia Sea. Polar Biol 40, 1229-1245.

MacLennan, D.N., Fernandes, P., Dalen, J., 2002. A consistent approach to definitions and symbols in fisheries acoustics. ICES J. Mar. Sci. 59, 365–369.

Maiti, K., Charette, M.A., Buesseler, K.O., Kahru, M., 2013. An inverse relationship between production and export efficiency in the Southern Ocean. Geophys. Res. Lett. 40, 1557–1561. https://doi:10.1002/grl.50219

Martin, A., Boyd, P., Buesseler, K., et al., 2020. The oceans' twilight zone must be studied now, before it is too late. Nature. 580. 26-28. https://doi:10.1038/d41586-020-00915-7

Mauchline, J., Fisher, L.R., 1969. The biology of euphausiids. Adv. Mar. Biol. 7, 1–454.

Meillat, M., 2012. Essais du chalut mésopélagos pour le programme MYCTO 3D - MAP de l'IRD, à bord du Marion Dufresne (du 10 au 21 août 2012). Rapport de mission, Ifremer.

Mongin, M., Molina, E., Trull, T.W., 2008. Seasonality and scale of the Kerguelen Plateau phytoplankton bloom: a remote sensing and modeling analysis of the influence of natural iron fertilization in the Southern Ocean. Deep-Sea Res. Part II. 55, 880–892. http://dx.doi.org/10.1016/j.dsr2.2007.12.039.

Nishikawa, J., Tsuda, A., 2001. Diel vertical migration of the tunicate *Salpa thompsoni* in the Southern Ocean during summer. Polar Biol. 24, 299-302

Pakhomov, E.A., Perissinotto, R., McQuaid, C.D., 1994. Comparative structure of the macrozooplankton/micronekton communities of the Subtropical and Antarctic Polar Fronts. Mar. Ecol. Prog. Ser. 111, 155–169.

Pakhomov, E., Perissinotto, R., McQuaid, C., 1996. Prey composition and daily rations of myctophid fishes in the Southern Ocean. Mar. Ecol. Prog. Ser. 134, 1–14.

Pakhomov, E.A., Froneman, P.W., 1999. Macroplankton/micronekton dynamics in the vicinity of the Prince Edward Islands (Southern Ocean). Mar. Biol. 134, 501–515.

Pakhomov, E.A., Yamamura, O., Brodeur, R.D., Domokos, R., Owen, K.R., Pakhomova, L.G., Polovina, J., Seki, M., Suntsov, A.V., 2010. Report of the advisory panel on micronekton sampling inter-calibration experiment. PICES Scientific Report 38, 108.

Pauthenet, E., et al., 2018. Seasonal meandering of the polar front upstream of the kerguelen Plateau. Geophys. Res. Lett. 45, 9774–9781. doi:10.1029/2018GL079614

Pepin, P., 2013. Distribution and feeding of *Benthosema glaciale* in the western Labrador Sea: Fish–zooplankton interaction and the consequence to calanoid copepod populations. Deep Sea Res. Part I. 75, 119-134. doi:http://dx.doi.org/10.1016/j.dsr.2013.01.012

Perrot, Y., Brehmer, P., Habasque, J., Roudaut, G., Behagle, N., Sarré, A., Lebourges-Dhaussy, A., 2018. Matecho: An Open-Source Tool for Processing Fisheries Acoustics Data. Acoust. Aust. 46, 241–248.

Pugh, P.R., 1984. The diel migrations and distributions within a mesopelagic community in the Northeast Atlantic. 7. Siphonophores. Prog. Oceanogr. 13, 461–489.

Quéguiner, B., Blain, S., Trull, T., 2011. High primary production and vertical export of carbon over the Kerguelen Plateau as a consequence of natural iron fertilization in a high-nutrient, low-chlorophyll environment. In: Duhamel, G., Welsford, D. (Eds.), The Kerguelen Plateau: Marine Ecosystem and Fisheries. Société Française d'Ichtyologie, Paris, 169-174.

Ratnarajah, L., Nicol, S., Bowie, A.R., 2018. Pelagic Iron Recycling in the Southern Ocean: Exploring the Contribution of Marine Animals. Front. Mar. Sci. 5, 109. doi: 10.3389/fmars.2018.00109

Roe, H., Angel, M., Badcock, J., Domanski, P., James, P., Pugh, P., & Thurston, M., 1984. The diel migrations and distributions within a Mesopelagic community in the North East Atlantic. 1. Introduction and sampling procedures. Prog. Oceanogr. 13, 245-268.

Romero-Romero, S., Choy, C. A., Hannides, C. C. S., Popp, B. N., Drazen, J. C., 2019. Differences in the trophic ecology of micronekton driven by diel vertical migration. Limnol. Oceanogr. 64, 1473-1483. doi:10.1002/lno.11128

Ryan, T.E., Downie, R.A., Kloser, R.J., Keith, G., 2015. Reducing bias due to noise and attenuation in open-ocean echo integration data. ICES J. Mar. Sci., 72, 2482–2493.

Sato, K., Charrassin, J., Bost, C., Naito, Y., 2004. Why do macaroni penguins choose shallow body angles that result in longer descent and ascent durations? J. Exp. Biol. 207, 4057–4065.

Saunders, R.A., Fielding, S., Thorpe, S.E., Tarling, G.A., 2013. School characteristics of mesopelagic fish at South Georgia. Deep Sea Res. Part I. 81, 62-77. https://doi.org/10.1016/j.dsr.2013.07.007

Saunders, R.A., Hill, S.L., Tarling, G.A., Murphy, E.J., 2019. Myctophid Fish (Family Myctophidae) Are Central Consumers in the Food Web of the Scotia Sea (Southern Ocean). Front. Mar. Sci. 6, 530.

Savoye, N., Trull, T.W., Jacquet, S.H.M., Navez, J., Dehairs,F., 2008. ^{234}Th-based export fluxes during a natural iron fertilizationexperiment in the Southern Ocean (KEOPS), Deep-Sea Res. II, 55, 841–855.

Schaafsma, F.L., Cherel, Y., Flores, H. et al., 2018. Review: the energetic value of zooplankton and nekton species of the Southern Ocean. Mar. Biol. 165, 129. https://doi.org/10.1007/s00227-018-3386-z

Scheffer, A., Trathan, P.N., Edmonston, J.G., Bost, C.-A., 2016. Combined influence of meso-scale circulation and bathymetry on the foraging behaviour of a diving predator, the king penguin (*Aptenodytes patagonicus*). Prog. Oceanogr. 141, 1–16.

Skjoldal, H.R., Wiebe, P.H., Postel, L., Knutsen, T., Kaartvedt, S., Sameoto, D., 2013. Intercomparison of zooplankton (net) sampling systems: Results from the ICES/GLOBEC sea–going workshop. Prog. Oceanogr. 108, 1–42.

Trenkel, V., Berger, L., Bourguignon, S., Doray, M., Fablet, R., Massé, J., Mazauric, V., Poncelet, C., Quemener, G., Scalabrin, C., et al., 2009. Overview of recent progress in fisheries acoustics made by Ifremer with examples from the Bay of Biscay. Aquat. Living Ressour. 22, 433–445.

Wiebe, P.H., Chu, D., Kaartvedt, S., Hundt, A., Melle, W., Ona, E., Batta-Lona, P., 2010. The acoustic properties of *Salpa thompsoni*. ICES J. Mar. Sci. 67, 583–593.

Table 1. Summary of trawl samples.

Station	Visit	Date	Day/Night	Latitude (°S) /Longitude (°E)	Max depth (m)	Trawl ID
M1	1st	08/03/18	Night	49.85 / 74.90	29-51	21
		08/03/18	Night		248-290	22
		08/03/18	Night		576-617	23
		09/03/18	Day		367-400	24
		09/03/18	Day		21-50	25
		09/03/18	Day		611-632	26
M2	1st	26/02/18	Day	50.62 / 72.00	318	1
		26/02/18	Day		178-210	2
		26/02/18	Day		320-350	3
		27/02/18	Night		307-346	4
		27/02/18	Night		35-55	5
		27/02/18	Night		118-158	6
	2nd	07/03/18	Day		151-170	15
		07/03/18	Day		49-70	16
		07/03/18	Day		315-350	17
		07/03/18	Night		283-317	18
		07/03/18	Night		30-50	19
		07/03/18	Night		141-175	20
	3rd	16/03/18	Night		33-65	37
		16/03/18	Night		335-377	38
		16/03/18	Night		21-30	39
		17/03/18	Day		89-105	40
		17/03/18	Day		318-340	41
		17/03/18	Day		157-190	42
M3	1st	04/03/18	Day	50.68 / 68.06	29-55	13
		04/03/18	Day		423-460	14
	2nd	15/03/18	Day		609-683	33
		15/03/18	Night		591-610	34
		15/03/18	Night		72-90	35
		15/03/18	Night		368-415	36
	3rd	18/03/18	Day		772-814	43
		18/03/18	Day		547-600	44
		18/03/18	Day		47-65	45
		19/03/18	Night		777-802	46
		19/03/18	Night		611-650	47

		19/03/18	Night		51-73	48
M4	1st	01/03/18	Day	52.60 / 67.20	78-93	7
		01/03/18	Day		556-575	8
		01/03/18	Day		398-425	9
		02/03/18	Night		363-400	10
		02/03/18	Night		80-96	11
		02/03/18	Night		547-575	12
	2nd	14/03/18	Day		57-85	27
		14/03/18	Day		576-610	28
		14/03/18	Day		363-410	29
		14/03/18	Night		572-600	30
		14/03/18	Night		52-85	31
		14/03/18	Night		365-400	32

Table 2. Proportion and occurrence of gelatinous species caught during trawl operations. Main contributions are in bold (>50 % in occurrence and >3 % in relative frequency).

FAMILY	Species	% occurrence	% all stations	% M1	% M2	% M3	% M4
CHAETOGNATHS	*Sagitta gazellae*	**93.62**	0.77	0.43	0.62	3.56	1.34
CTENOPHORES	*Beroe cucumis*	31.91	0.89	0.75	0.21	2.33	2.95
	Bolinopsis sp.	29.79	0.74	0.24	0.09	**11.98**	0.09
	Leucothea sp.	2.13	0.01	0.00	0.00	0.17	0.00
MEDUSAE	*Atolla wyvillei*	17.02	1.53	0.62	0.00	**14.36**	**4.42**
	Calycopsis borchgrevinki	**51.06**	0.35	0.28	0.14	1.66	0.71
	Calycopsis sp. 2	6.38	0.02	0.00	0.00	0.31	0.00
	Halicreas minimum	2.13	0.00	0.00	0.00	0.05	0.00
	Haliscera conica	4.26	0.02	0.00	0.00	0.35	0.00
	Medusa unknown B	4.26	0.03	0.00	0.00	0.51	0.00
	Periphylla periphylla	29.79	1.02	0.05	0.19	**5.92**	**5.00**
	Rhopalonema sp.	2.13	0.01	0.00	0.00	0.00	0.05
	Scyphomedusae	2.13	0.05	0.00	0.00	0.00	0.40
	Solmissus sp. *(Medusa unknown A)*	36.17	0.37	0.27	0.00	1.38	1.47
	Stygiomedusa gigantea	0.00	0.00	0.00	0.00	0.00	0.00
NEMERTEANS	*Pelagonemertes rollestoni*	8.51	0.01	0.00	0.00	0.20	0.00
POLYCHAETES	*Tomopteris carpenteri*	17.02	0.01	0.01	0.02	0.03	0.00
SALPS	*Salpa thompsoni*	**85.11**	**73.63**	**89.74**	**86.88**	**10.63**	**2.75**
SIPHONOPHORES	*Diphyes* sp.	4.26	0.00	0.00	0.00	0.01	0.00
	Rosacea plicata	**55.32**	**20.59**	**7.60**	**11.85**	**46.55**	**80.83**

Table 3. Proportion and occurrence of crustaceans species caught during trawl operations. Main contributions are in bold (>50 % in occurrence and >3 % in relative frequency).

FAMILY	Species	% occurrence	% all stations	% M1	% M2	% M3	% M4
EUPHAUSIIDS	*Euphausia longirostris*	10.64	0.30	1.85	0.00	0.00	0.00
	Euphausia triacantha	**82.98**	**11.28**	**15.71**	**7.20**	**20.03**	**9.99**
	Euphausia vallentini	**87.23**	**43.12**	**43.28**	**28.16**	**41.55**	**74.39**
	Thysanoessa macrura/vicina	**51.06**	2.78	**4.99**	2.67	0.06	**3.30**
GAMMARID AMPHIPODS	*Cyphocaris richardi*	31.91	0.12	0.01	0.00	0.22	0.39
	Danaela mimonectes	10.64	0.01	0.00	0.00	0.01	0.02
	Eurythenes obesus	6.38	0.00	0.01	0.00	0.01	0.00
	Eusiroides stenopleura	19.15	0.03	0.02	0.00	0.10	0.07
	Parandania boecki	40.43	0.89	1.55	0.08	2.22	1.11
HYPERIID AMPHIPODS	*Cyllopus magellanicus*	**80.85**	0.87	2.27	0.89	0.25	0.24
	Hyperia spinifera	12.77	0.01	0.01	0.01	0.01	0.00
	Hyperia macrocephala	6.38	0.00	0.00	0.01	0.00	0.00
	Hyperiella antarctica	2.28	0.01	0.01	0.01	0.03	0.01
	Hyperoche luetkenides	44.68	0.07	0.11	0.09	0.03	0.02
	Pegohyperia princeps	2.13	0.00	0.00	0.00	0.00	0.00
	Physosomata sp. 1	6.38	0.00	0.00	0.00	0.02	0.00
	Physosomata sp. 2	4.26	0.00	0.01	0.00	0.00	0.00
	Primno macropa	**87.23**	1.65	2.07	1.52	**3.44**	0.44
	Scinidae sp.	0.00	0.00	0.00	0.00	0.00	0.00
	Themisto gaudichaudii	**100.00**	**37.77**	**25.49**	**59.06**	**29.42**	**9.68**
	Vibilia antarctica	**72.34**	0.59	2.44	0.25	0.40	0.05
MYSIDS	*Neognathophausia gigas*	8.51	0.01	0.00	0.00	0.04	0.00
	Mysida sp.	17.02	0.25	0.00	0.05	1.44	0.00
	Mysida sp. (red)	4.26	0.04	0.00	0.00	0.27	0.00
NATANTIA	*Acanthephyra pelagica*	4.26	0.00	0.00	0.00	0.01	0.00
	Campylonotus sp. (red)	21.28	0.01	0.02	0.00	0.03	0.00
	Pasiphaea scotiae	25.53	0.04	0.03	0.00	0.08	0.09
	Gennada sp./Natantia sp.	6.38	0.01	0.01	0.00	0.03	0.00
	Sergestidae sp.	6.38	0.01	0.03	0.00	0.00	0.00
	Decapoda larvae	10.64	0.01	0.02	0.00	0.02	0.00
OSTRACODS	*Gigantocypris muelleri*	21.28	0.10	0.07	0.00	0.30	0.19

Table 4. Proportion and occurrence of fish species caught during trawl operations. Main contributions are in bold (>40 % in occurrence and >3 % in relative frequency).

FAMILY	Species	% occurrence	% all stations	% M1	% M2	% M3	% M4
BATHYLAGIDAE	*Bathylagus tenuis*	23.40	**5.52**	**3.58**	0.00	**7.94**	**4.69**
GONOSTOMATIDAE	*Cyclothone* sp. A	25.53	**3.18**	0.68	0.00	2.65	**6.93**
	Cyclothone sp. B	2.13	0.06	0.00	0.00	0.13	0.00
STOMIIDAE	*Stomias boa/gracilis*	21.28	0.83	1.87	0.00	0.97	0.22
ASTRONESTHIDAE	*Borostomias antarcticus*	2.13	0.03	0.00	0.00	0.06	0.00
IDIACANTHIDAE	*Idiacanthus atlanticus*	2.13	0.03	0.17	0.00	0.00	0.00
SCOPELARCHIDAE	*Bentalbella macropinna*	8.51	0.18	0.17	0.00	0.06	0.45
PARALEPIDIDAE	*Notolepis coatsi*	**48.94**	3.03	1.70	**12.20**	1.87	2.46
MYCTOPHIDAE	*Electrona antarctica*	**65.96**	**27.71**	**29.64**	**37.50**	**17.62**	**40.22**
	Electrona subaspera	2.13	0.03	0.17	0.00	0.00	0.00
	Gymnoscopelus bolini	2.13	0.03	0.00	0.00	0.06	0.00
	Gymnoscopelus braueri	**44.68**	**4.07**	**3.24**	2.68	**5.62**	2.46
	Gymnoscopelus fraseri	4.26	0.27	0.00	0.60	0.00	0.78
	Gymnoscopelus nicholsi	14.89	0.27	0.17	1.79	0.06	0.11
	Krefftichthys anderssoni	**55.32**	**28.10**	**20.61**	**18.15**	**41.06**	**14.30**
	Krefftichthys anderssoni (postlarvae)	**55.32**	**21.18**	**32.54**	**4.17**	**18.85**	**24.13**
	Nannobrachium achirus	8.51	0.39	0.00	0.00	0.65	0.34
	Protomyctophum andriashevi	4.26	0.12	0.68	0.00	0.00	0.00
	Protomyctophum bolini	38.30	1.54	1.19	**6.55**	0.19	2.23
	Protomyctophum gemmatum	2.13	0.03	0.17	0.00	0.00	0.00
	Protomyctophum parallelum	4.26	0.06	0.00	0.00	0.13	0.00
	Protomyctophum tenisoni	19.15	0.45	0.85	2.38	0.13	0.00
	Myctophidae (postlarvae)	4.26	0.09	0.00	0.00	0.19	0.00
MURAENOLEPIDAE	*Muraenolepis marmoratus*	27.66	0.83	0.51	**5.95**	0.26	0.11
MACROURIDAE	Macrouridae sp.	2.13	0.03	0.00	0.00	0.06	0.00
MELANONIDAE	*Melanonus gracilis*	4.26	0.12	0.51	0.00	0.06	0.00
MELAMPHAIDAE	*Poromitra crassiceps*	2.13	0.33	0.00	0.00	0.71	0.00
LIPARIDAE	*Paraliparis thalassobathyalis*	2.13	0.03	0.00	0.00	0.06	0.00
NOTOTHENIIDAE	*Notothenia rossii* (blue fingerling)	10.64	0.18	0.00	0.89	0.19	0.00
	Postlarvae type A	25.53	0.95	1.53	**6.55**	0.06	0.00
GEMPYLIDAE	*Paradiplospinus gracilis*	4.26	0.06	0.00	0.60	0.00	0.00
ACHIROPSETTIDAE	*Achiropsetta tricholepis*	6.38	0.12	0.00	0.00	0.26	0.00
Larvae (unidentified)		6.38	0.18	0.00	0.00	0.06	0.56

Table 5. Comparison of migrant biomass (MB), respiratory carbon flux (RCF) and total carbon fluxes (TCF) estimated in this study and in other regions for myctophids (except in Kwong et al. (2020) estimation for micronekton including myctophids, decapods, and cephalopods). Mechanism included to compute the TCF are annotated with the following letters: R (respiration), D (defecation), E (excretion), and M (mortality). Temperature refers to the residence depth of myctophids during daytime according to the authors.

Source	Location	Temperature (°C)	Site	MB (mg C m⁻² d⁻¹)	RCF (mg C m⁻² d⁻¹)	TCF (mg C m⁻² d⁻¹)
This study[a§]	Kerguelen Islands	2.2	Productive downstream (M1)	1.676	0.043	0.087[RDM]
		2.2	Productive on Plateau (M2)	1.761 (0.041 - 5.937)	0.004 (0.001 – 0.012)	0.009 (0.001 – 0.026)[RDM]
		2.2	HNLC upstream, north of PF (M3)	1.255 (0.201 - 2.309)	0.005 (0.001 - 0.008)	0.009 (0.002 – 0.016)[RDM]
		2.2	HNLC upstream, south of PF (M4)	10.072 (5.067 - 15.077)	0.031 (0.016 - 0.045)	0.061 (0.032 – 0.091)[RDM]
Kwong et al. (2020)[a§]	Southeast Australia	10-20	Cold core eddy "B-CCE"	0.5	0.17	0.38[RDEM]
		10-20	Warm core eddy "R-WCE"	4.1	0.56	1.53[RDEM]
		10-20	Warm core eddy "W-CE"	10.6	2.75	6.71[RDEM]
Belcher et al. (2019)[a‡]	Scotia Sea	2	JR 161 WSS	49.8	0.05	-
		2	JR161 NSS	520.6	0.28	-
		2	JR177 GB	238.5	0.13	-
		2	JR177 MSS	407.1	0,33	-
Ariza et al. (2015)[b†]	Canary Islands	12	North of Gran Canaria	168	2.68	-
Hudson et al. (2014)[b†]	North Azores	6.x	Reykjanes Rdige	5.2	0.005-0.027	-
		11.8	Azorean Zone	40	0.046-0.271	-
Hidaka et al. (2001)[b§]	Western equatorial Pacific	9.3	Station 15	462.5	1.98	2.16[RDM]
		9.3	Station 16	248.9	1.06	1.17[RDM]
		9.3	Station 8	539.5	2.31	2.53[RDM]
		9.3	Station 10	406.5	1.74	1.90[RDM]
		9.3	Station 13	726.92	3.07	3.36[RDM]

aUncorrected for capture efficiency
bAssumes 14% of capture efficiency
†Small framed trawl
‡Medium framed trawl
§Large pelagic trawl

Fig. 1. Location of the study area in the polygon (black line) with the main oceanographic features, i.e. the Antarctic circumpolar current (ACC) and the main circumpolar fronts, the polar front (PF), the subantarctic front (SAF) and the Subtropical front (STF) (upper panel), and locations of the four stations (M1, M2, M3 and M4) in the Kerguelen region during the MOBYDICK survey (lower panel). Acoustic and trawl data areas are indicated by blue squares. The dotted line indicates the mean location of the Polar Front during the study period.
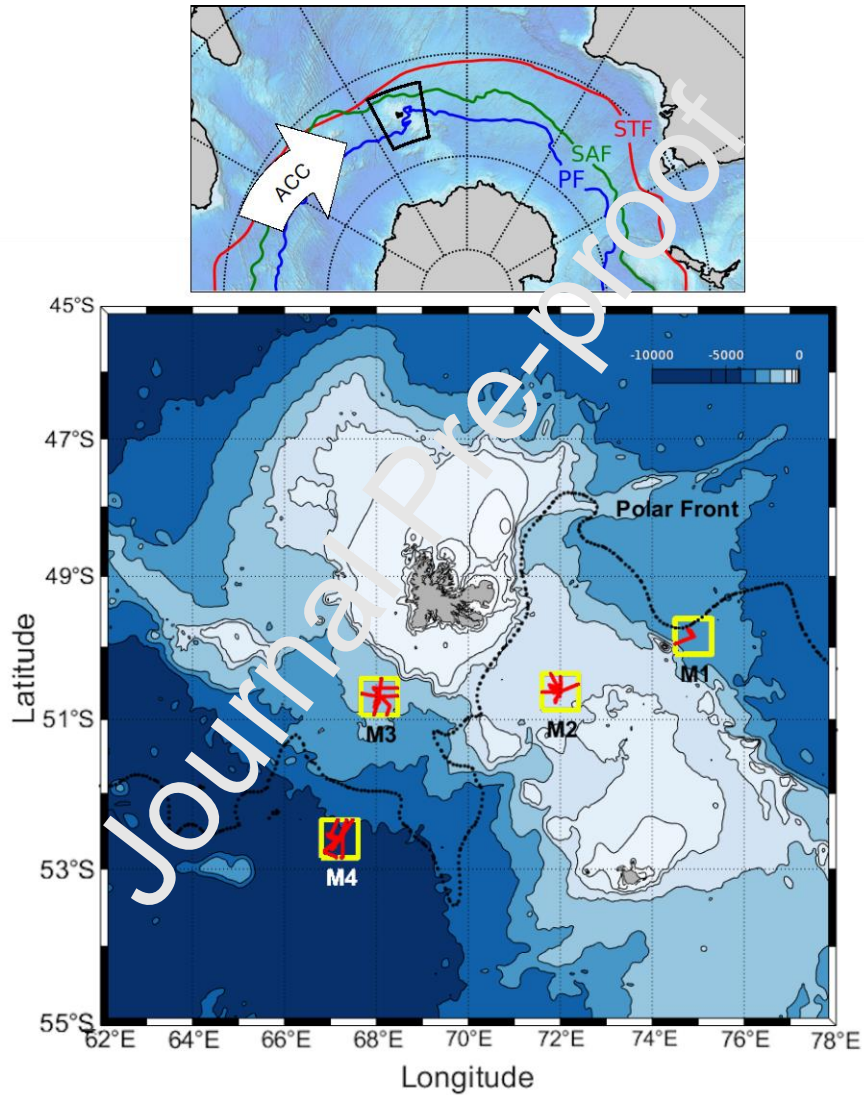
Fig. 2. Time series of weekly-averaged chlorophyll a concentration (mg m^{-3}) at each MOBYDICK station (blue squares in Figure 1) from October 2017 to March 2018.
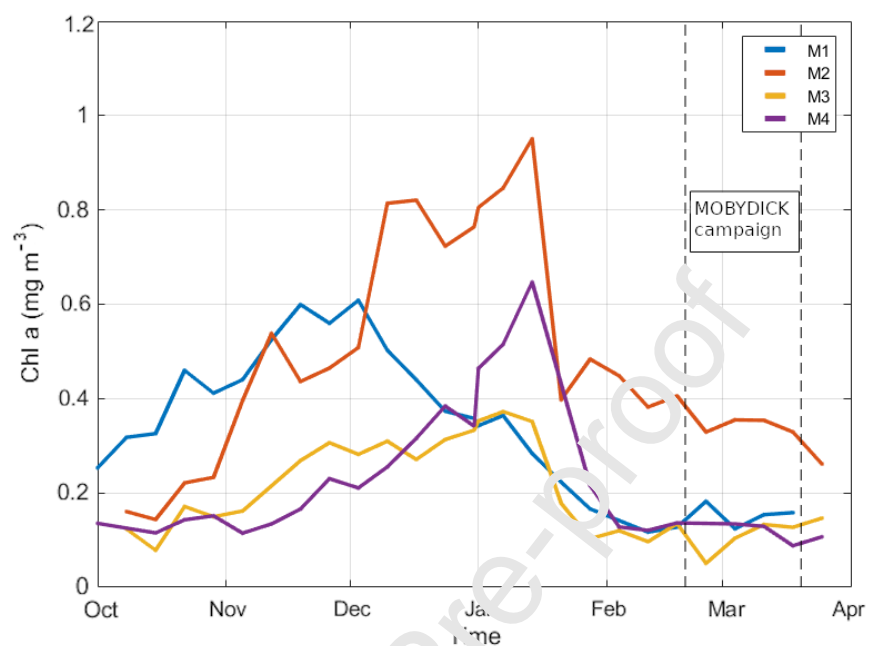
Fig. 3. Night-day (left-right) absolute wet biomass (in g 1000 m^{-3}) of macrozooplankton-micronekton from trawls.
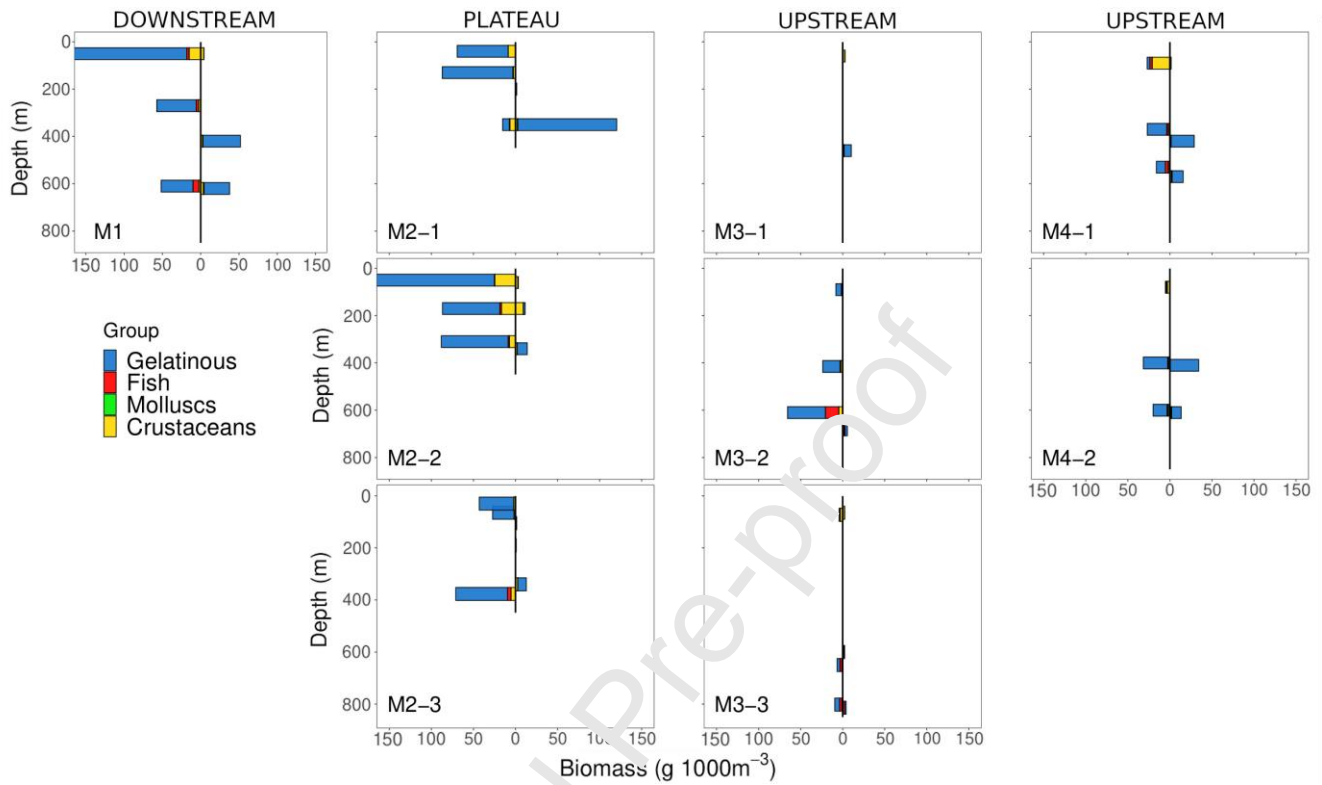
Fig. 4. Night-day (left-right) absolute wet biomass (in g 1000 m^{-3}) of the main gelatinous organisms from trawls.
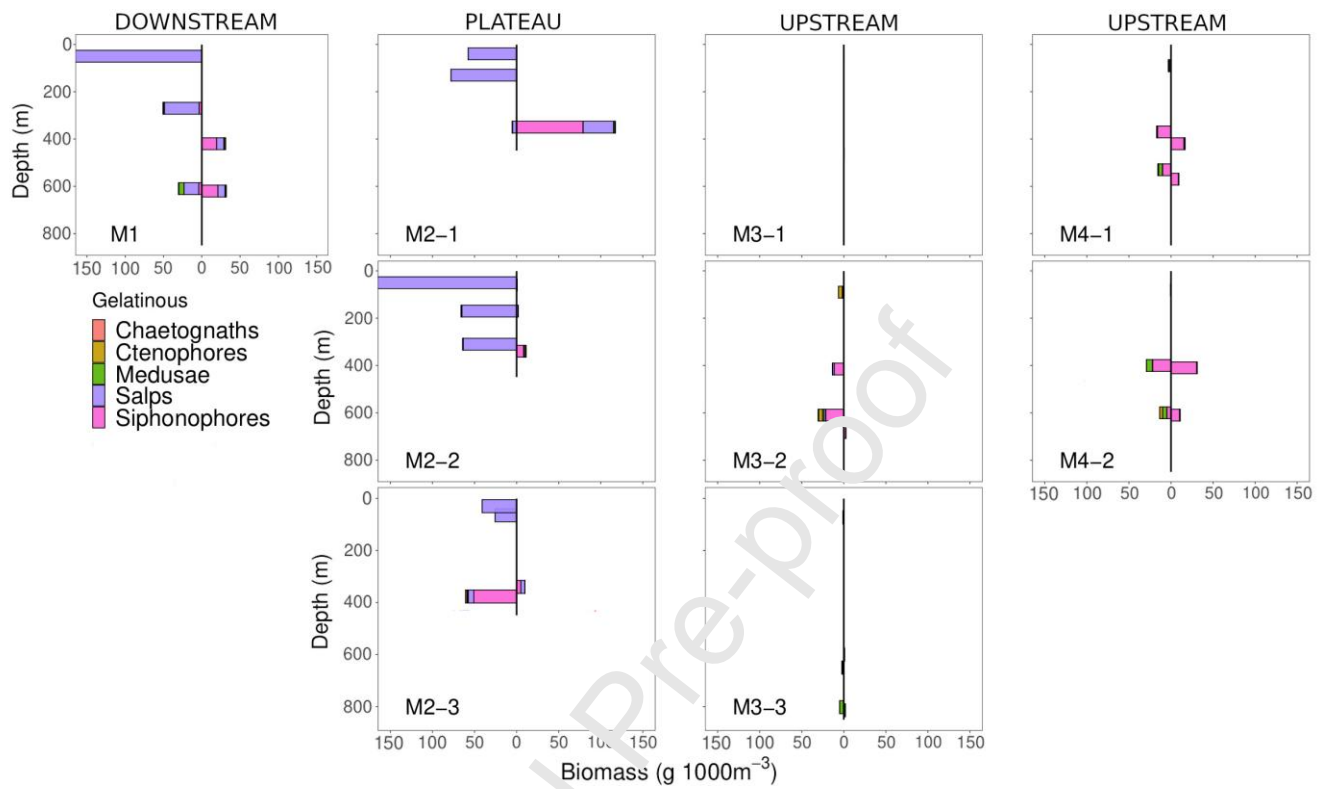
Fig. 5. Night-day (left-right) absolute abundance (in individual 1000 m^{-3}) of the main crustaceans from trawls.
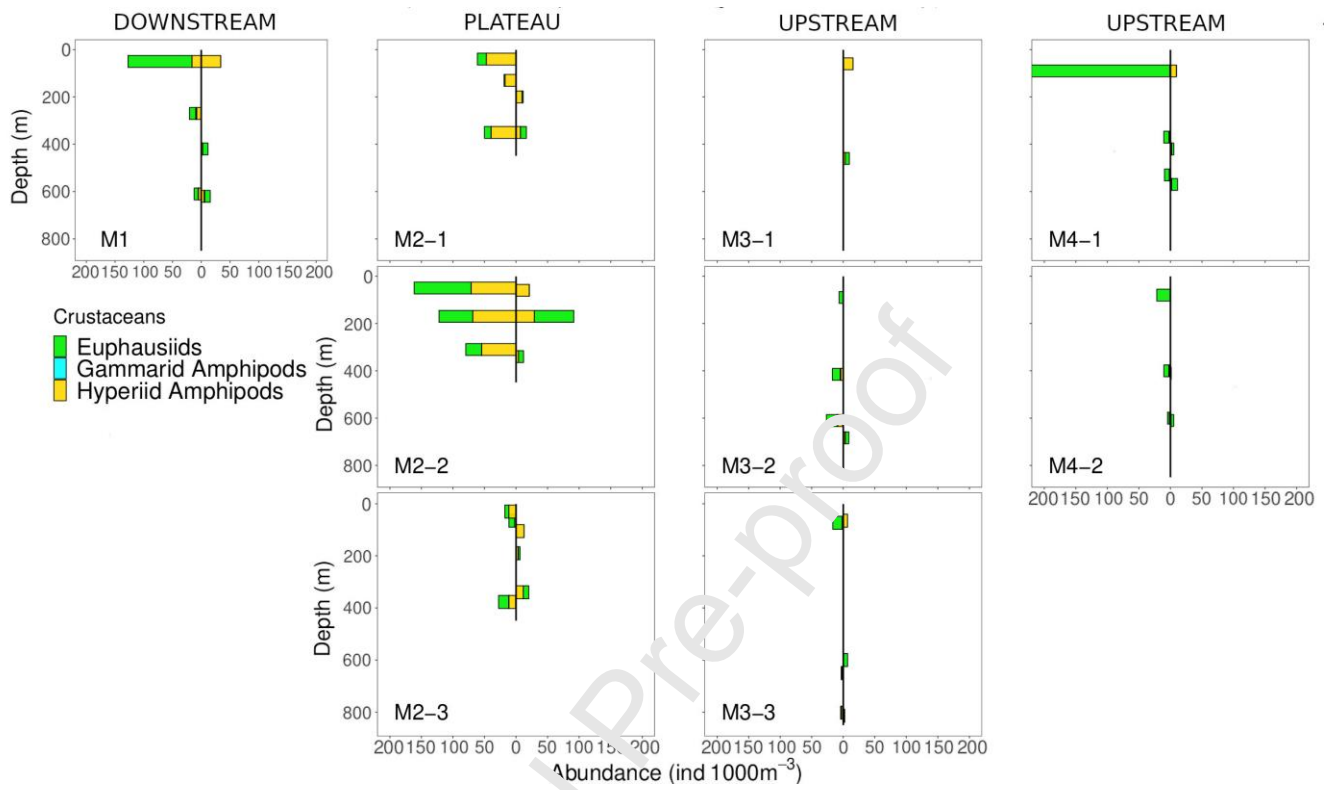
Fig. 6. Night-day (left-right) absolute abundance (in individual 1000 m^{-3}) of the main myctophids from trawls.
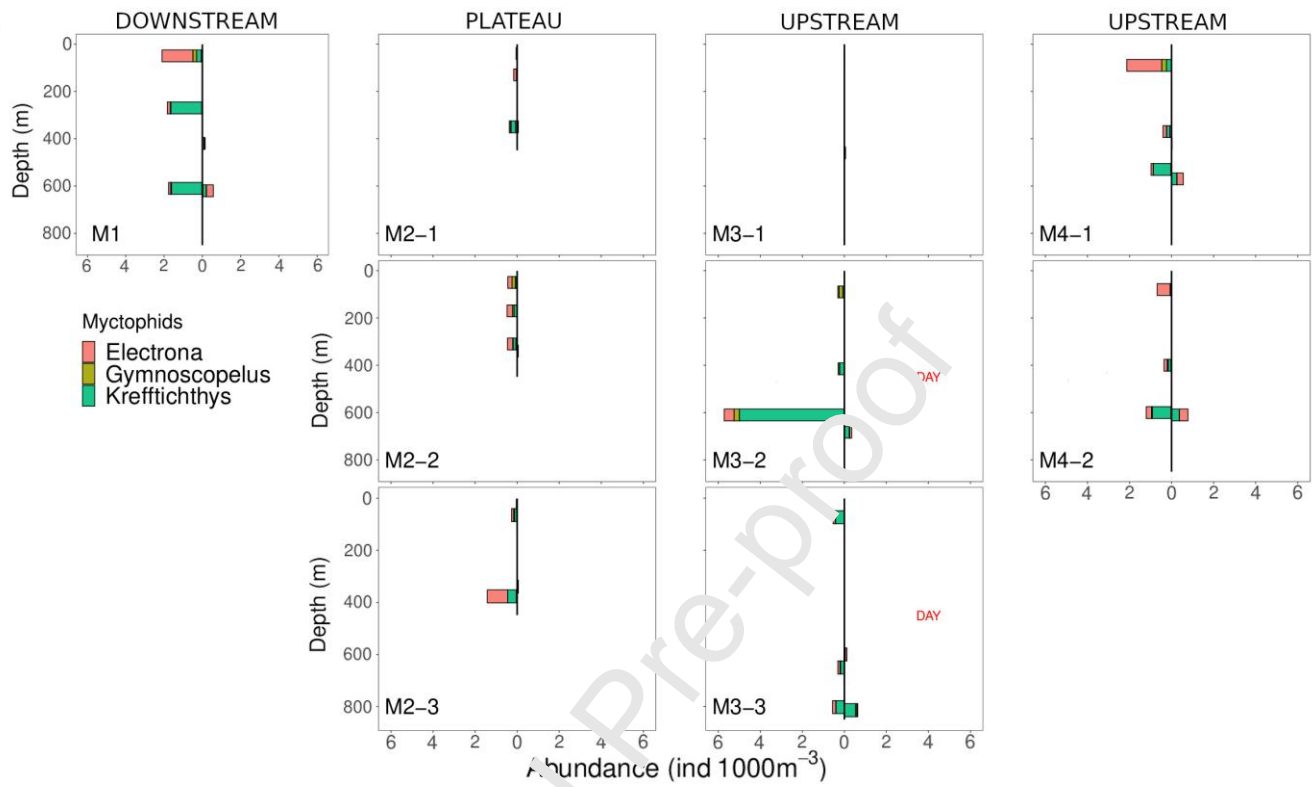
Fig. 7. Night-day (left-right) mean vertical NASC profiles at 18kHz (red) and 38 kHz (blue).
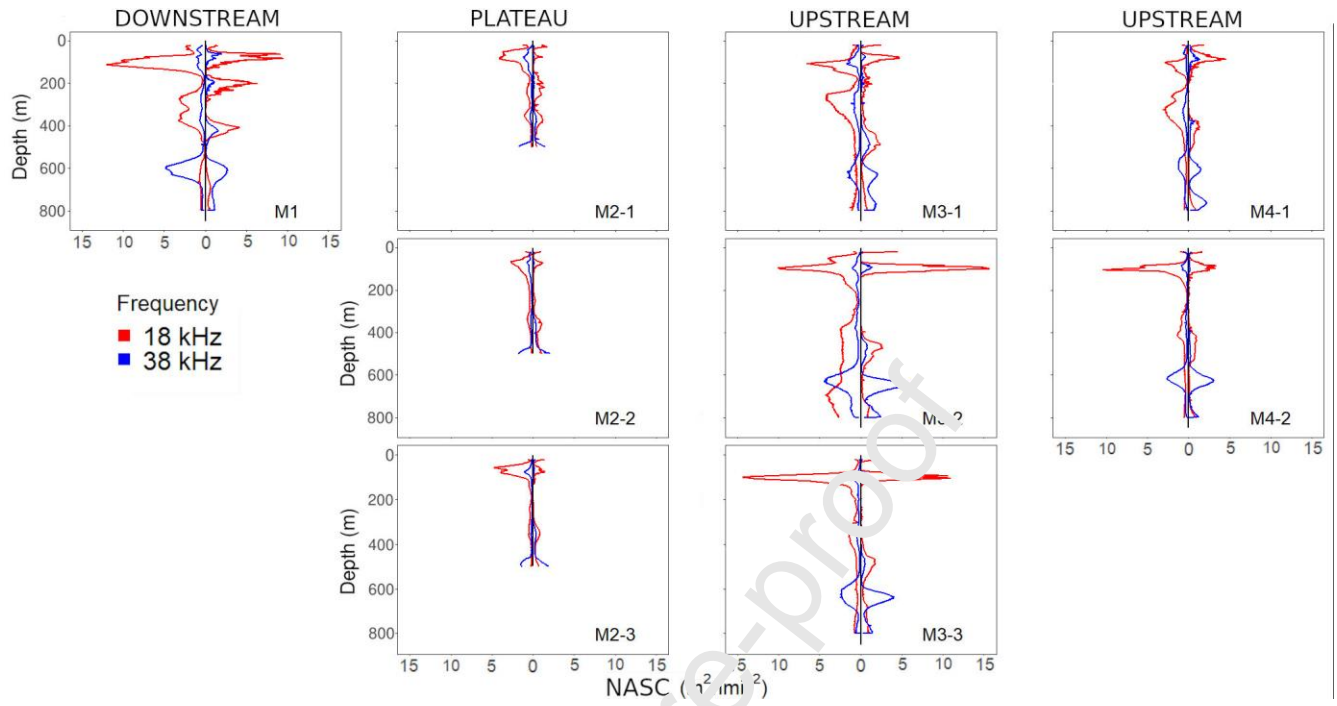
Fig. 8. Daily RGB composites of Sv values (dB re $1m^{-1}$) from 12 to 800m for the four stations, with the 18 kHz displayed in red and the 38 kHz frequency displayed both in green and blue.
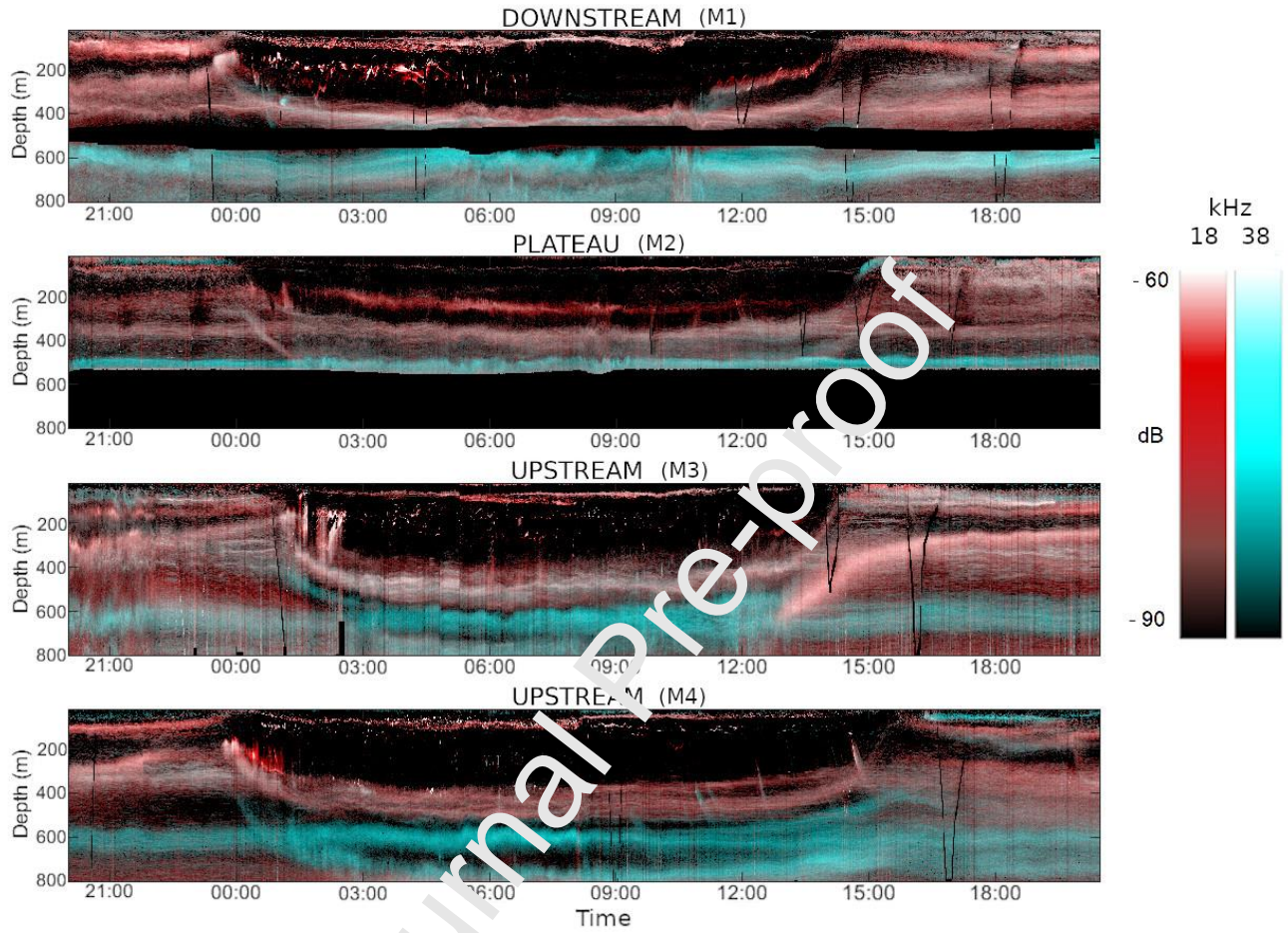
Fig. 9. Night-day (left-right) carbon content (in mg m^{-3}) of macrozooplankton-micronekton from trawls.
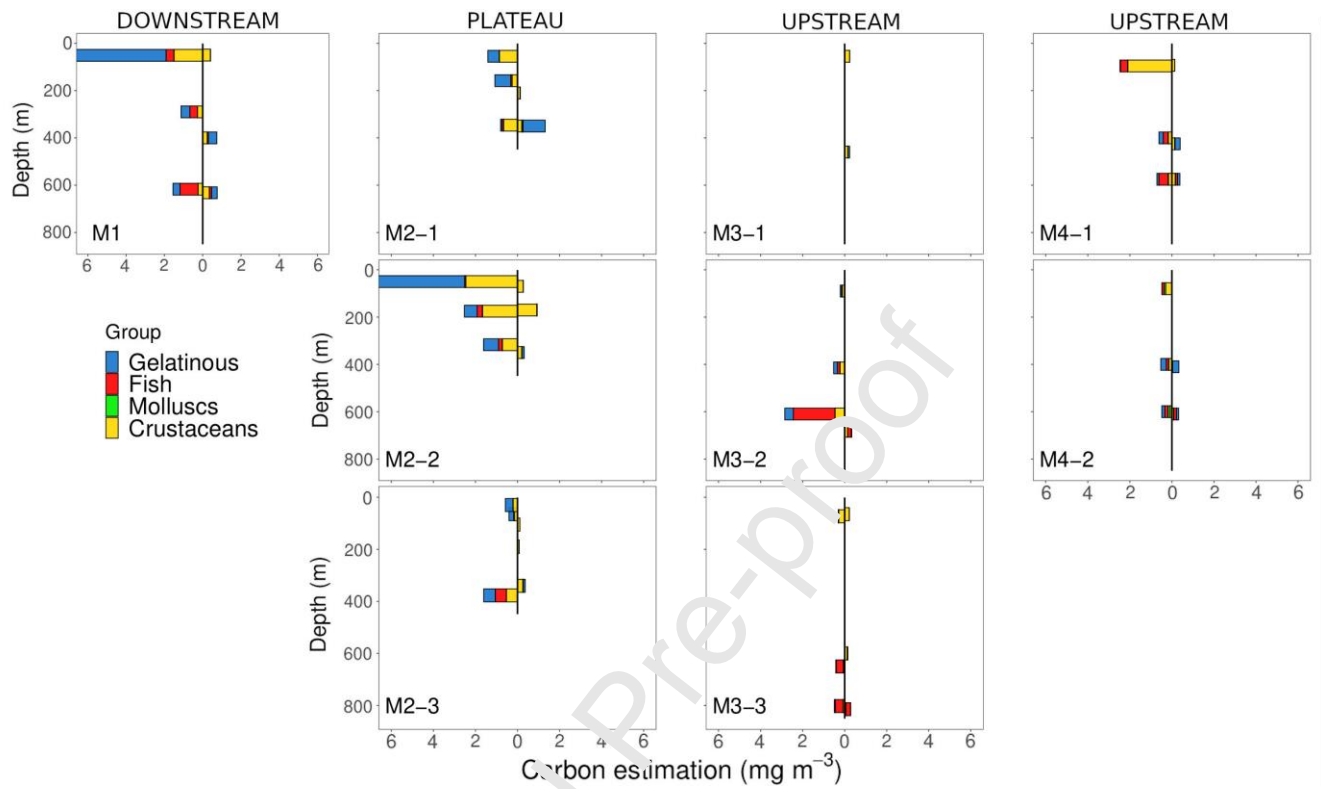
Fig. 10. Averaged chlorophyll *a* from 20 to 100 m depth (a-d), depth range of trawling used to target the migrant layers in the 200 m surface scattering layer (grey boxes) and mixed layer depth (dashed line) at each visit (e-h), and migrant abundance (i-j), biomass (m-p) and carbon flux (q-t) mediated by fish from the family Myctophidae, through respiration, defecation, and mortality at depth.
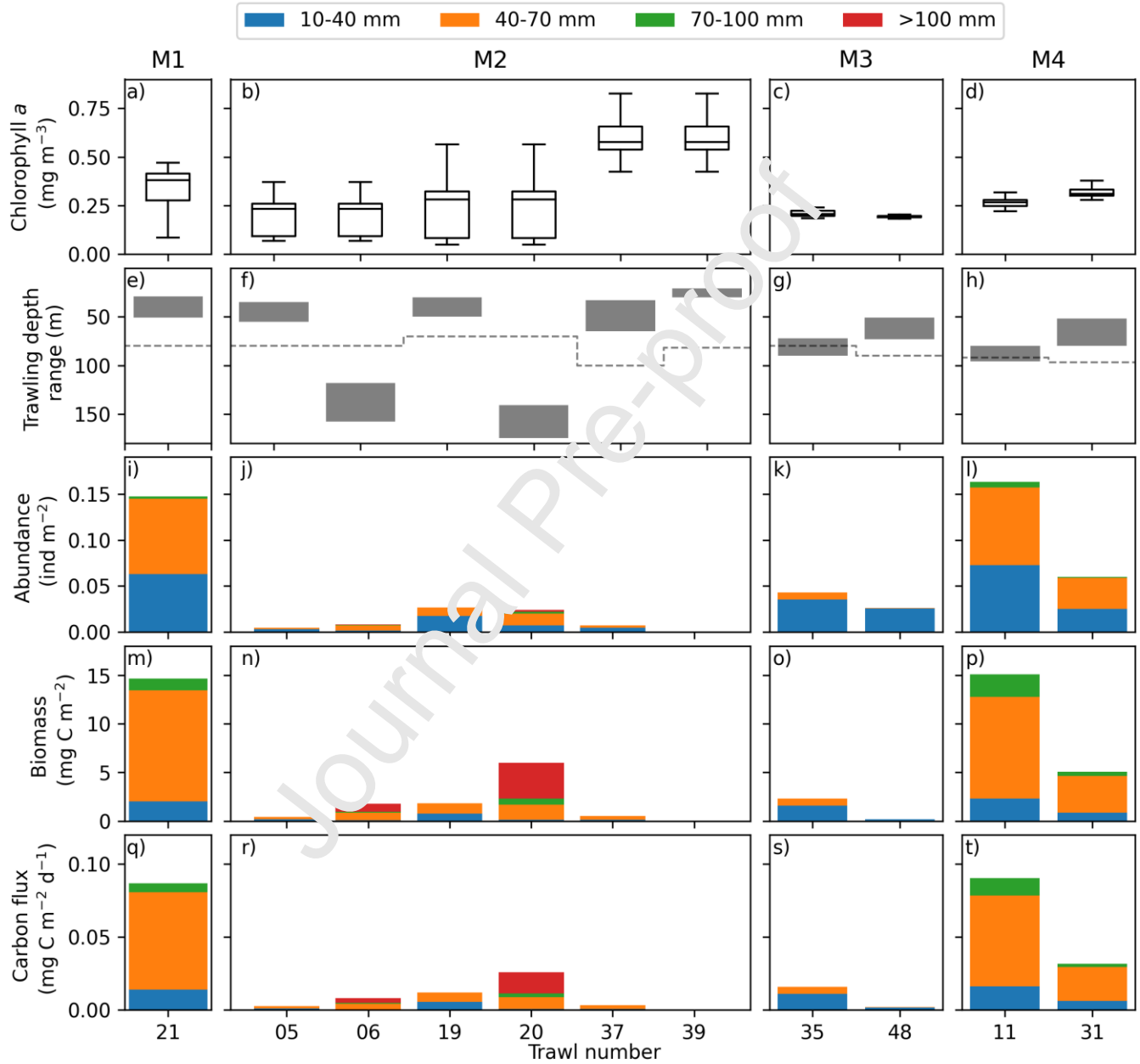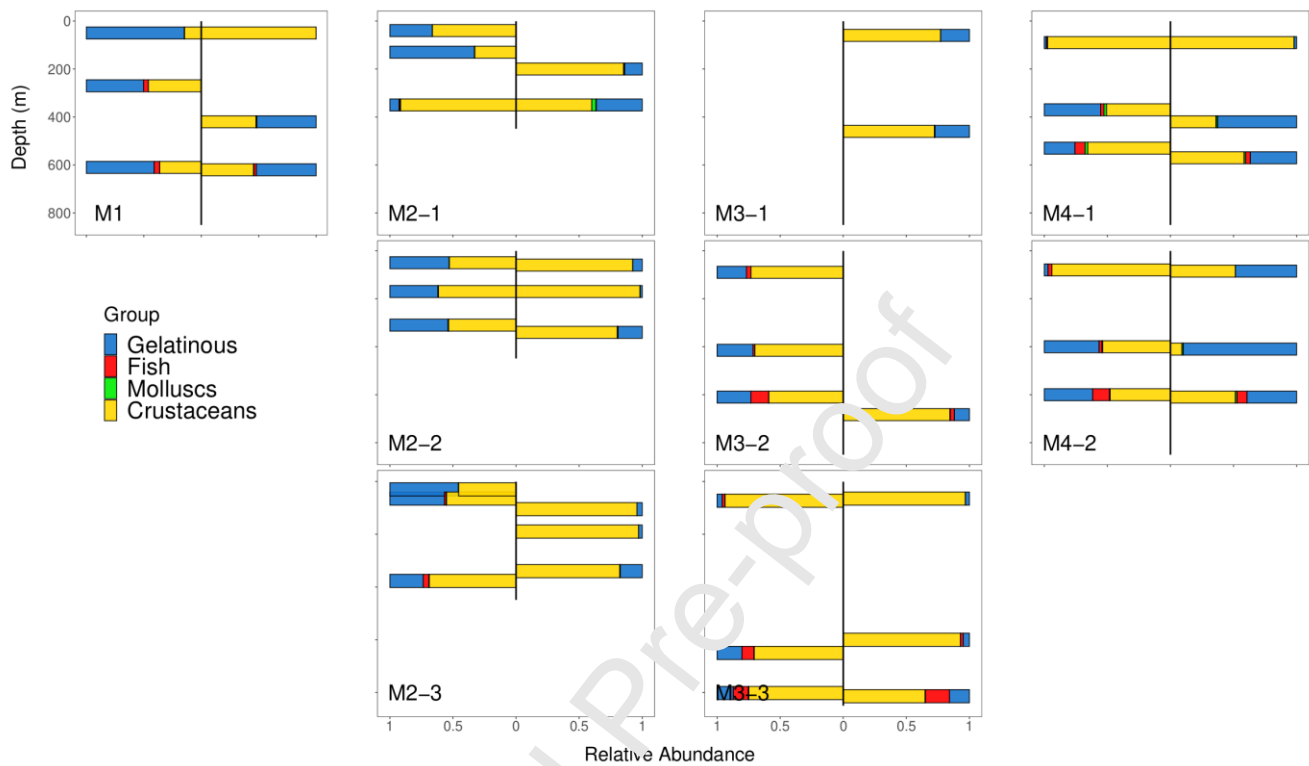
Supplementary material 1

Night-day (left-right) relative wet biomass of macrozooplankton-micronekton from trawls.
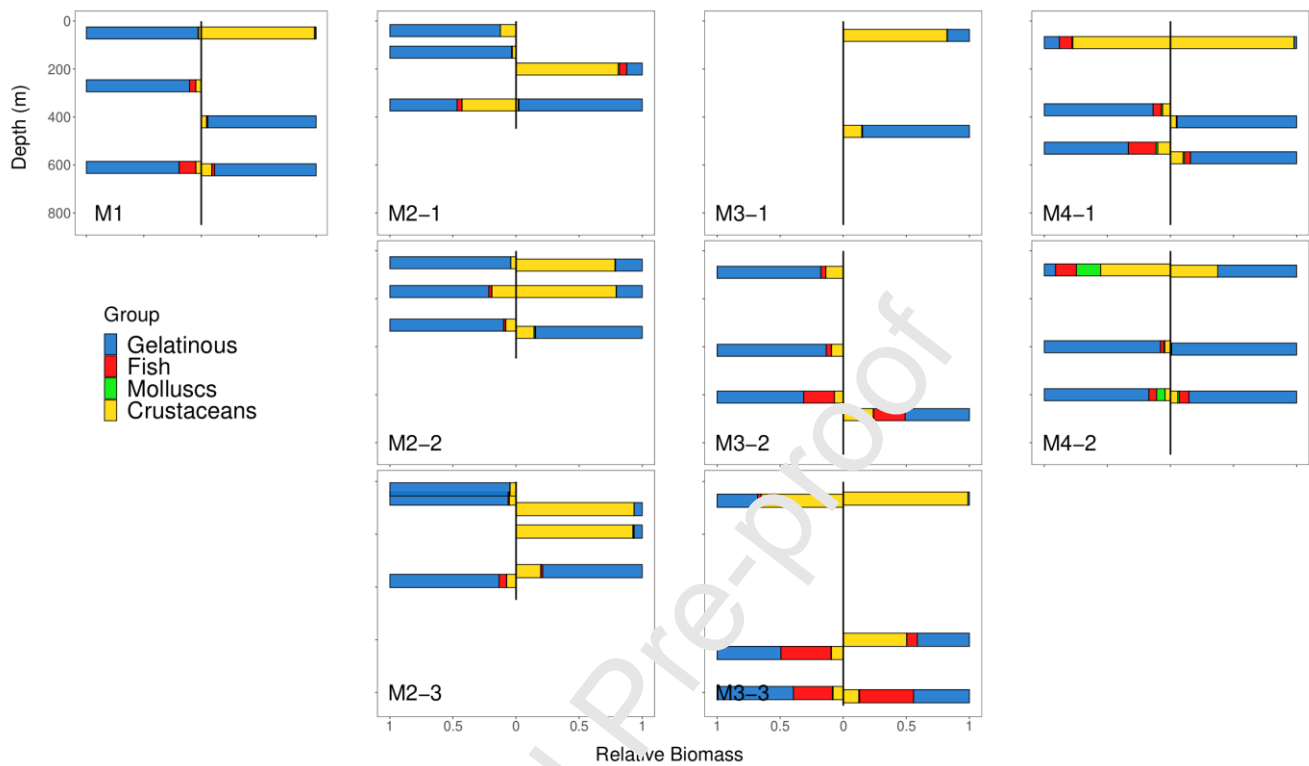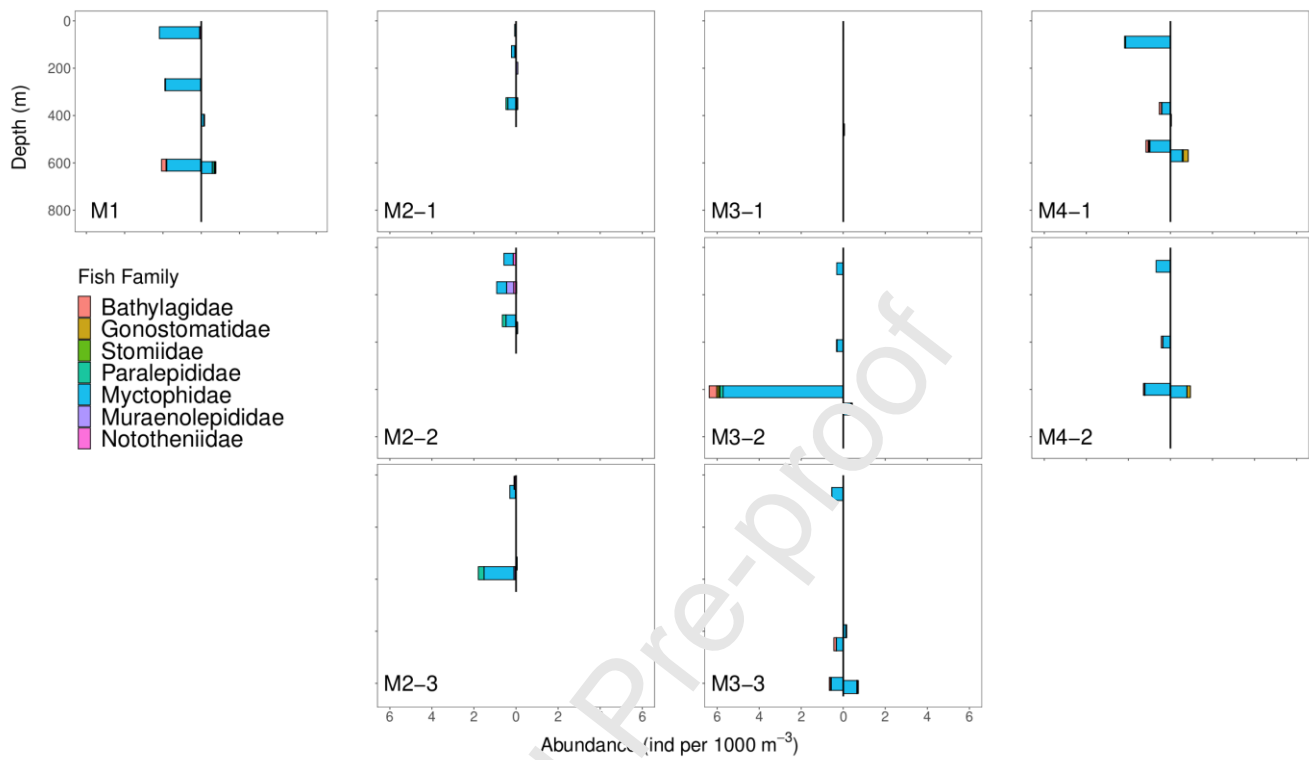
Supplementary material 2

Night-day (left-right) relative abundance of macrozooplankton-micronekton from trawls.

Supplementary material 3

Night-day (left-right) absolute abundance (in individual 1000 m^{-3}) of fish from trawls.

Supplementary material 4

Size frequency densities for the two main fish species per station and depth strata.

Highlights

- This Study reports a detailed description of the macrozooplankton and micronekton communities in the Kerguelen area using trawl and two-frequency acoustic data
- We depict a consistent three-layers system observed between the surface and 800 m over the Kerguelen seascape (Chlorophyll biomass, Polar Front position) but different assemblages
- Salps was dominant in terms of biomass in the productive areas and scarce in HNLC region while crustaceans were abundant on the Plateau
- Myctophids were prominent below 400m where they formed permanent or migrant layers accounting for the main source of carbon biomass
- We estimate total carbon flux mediated by migratory myctophids in the contrasting productive areas